Ali El Rifai

Grid Codes Certification by Simulation

School of Technology and Innovations
Master's thesis in Smart Energy programme

Vaasa 2024

UNIVERSITY OF VAASA
School of innovation Technology
Author: Ali El Rifai
Title of the thesis: Grid Codes certification by simulation
Degree: Master of Science in Technology
Programme: Smart Energy
Supervisors: Mustafa Alrayah Hassan Ibraheem
Instructor: Muhammad Khurram Shahzad
Evaluator: Kimmo Kauhaniemi
Year: 2024 **Pages: 92**

ABSTRACT:

Reliance on fossil fuels as the primary source of energy has led to a significant rise in greenhouse emissions, which has become an environmental threat. Therefore, there has been an increasing trend towards utilizing alternative inverter-based distributed energy resources in recent years. Incorporating distributed energy resources is the key to a sustainable energy sector. However, integrating distributed energy sources into the grid presents a major challenge because of their fluctuating and intermittent nature, which can lead to grid instability. Therefore, grid codes and standards have been developed to ensure the reliability and safety of the grid.

The current certification tests and on-site commissioning are costly, time-consuming, and may not cover all grid code requirements. In addition, compliance certification tests by a third party within a short time are highly required. Therefore, simulation tests help bridge the gap between their type tests and on-site tests. This study aims to establish standardized, efficient compliance testing for grid code simulation using MATLAB Simulink. By improving the testing process and narrowing the gap between type tests and on-site testing, this thesis paves the way.

This master's thesis provides a method for testing grid code compliance based on EN50549-1, EN50549-2, and EN50549-10 standards. The study focuses on key aspects such as under voltage-ride-through and over-voltage ride-through. Two grid code tests were conducted by MATLAB Simulink. The first test assesses the ability of the inverter to withstand over-voltage and under-voltage events, by dividing the OVRT and UVRT curves into three zones and then creating voltage rise and dip scenarios. Two tests were conducted for each zone, and the simulation model showed that the inverter is compatible with the standards. The second test evaluates the compatibility of the inverter with frequency variations. The test was conducted by increasing the frequency to a value higher than the acceptable thresholds to ensure that the frequency relay would operate and disconnect the grid. The model was executed in real-time using the OPAL-RT simulator, and related grid code compliance testing conducted using HIL system was highlighted in this master thesis.

KEYWORDS: Grid codes Compliance, Under Voltage Ride Through, Over Voltage Ride Through, hard-ware-in-the-loop, Distributed energy resources

Acknowledgments

This thesis is done for Danfoss Drives Oy. Danfoss is an engineering technology that aims to bring more products to the world with the promise of reliability, innovation, and quality. Danfoss offers many products across their business segments: Danfoss Climate Solutions, Danfoss Drives, and Danfoss Power Solutions. Danfoss is a leading technology partner for customers who care about reducing carbon emissions in the world by increasing energy efficiency and machine productivity for a better future.

Firstly, a special thanks to Professor Kimmo Kauhaniemi for giving me this opportunity to write this master thesis. The journey in which I have gained valuable learning experience.

I am grateful to my personal supervisors, Mustafa Alrayah Hassan Ibraheem from the University of Vaasa, and my instructor from Danfoss Oy Muhammad Khurram Shahzad, for their guidance and support during this journey. And thanks to Aushiq Ali Memon for his help during this process.

I would like to express my gratitude to my family for their support during my academic journey.

Contents

Figures

Tables

Abbreviations

AC	Alternating Current
CLC/TC 8X	System aspects of electrical energy supply
C-HIL	Controller Hardware in Loop
DC	Direct Current
DR	Distributed generation
DSP	Digital Signal processing
EUT	Equipment under test
eHS	Electrical Hardware Solution
ESS	Energy storage system
FRT	Fault ride through
FPGA	Field Programmable Gate Arrays
HIL	Hardware-in-the-Loop
IPC	Interprocessor communication
LFSM-O	Frequency Sensitive Mode - Over frequency
MV	Medium Voltage
OVRT	Over voltage ride through
OVRC	Over voltage range capability
PV	Photovoltaic
PI	Proportional controller
PLL	Phase-locked loop
PGU	Power Generating Unit
POC	Point of connection
P-HIL	Power Hardware-in-the-Loop
RES	Renewable energy sources
RFG	Requirements for generators
ROCOF	Rate of change of frequency
SIL	Software-in-the-loop
TSO	Transmission system operator
UVRT	Under voltage ride through
UVRC	Under voltage range capability

1 Introduction

The utilization of fossil fuels such as oil and natural gas as a main source of energy raises a significant environmental concern (Khan et al., 2021). Therefore, electricity generation is experiencing a rapid shift towards power inverter systems and renewable energy resources.

Renewable sources are called clean energy sources as they rely on natural sources to produce energy; therefore, they are considered environmentally friendly. These resources reduce carbon dioxide emissions into the atmosphere resulting from fuel combustion. They also have other advantages, such as increasing the stability of the grid and providing the ability to produce and store electrical energy using an energy storage system (ESS) and then utilizing it during peak periods, which also helps reduce electricity bills (Vyas et al., 2023).

Consequently, the installation capacity of renewable energy resources such as wind turbines and solar panels has increased remarkably, especially during the last ten years (Rafiq et al., 2022). Figure 1 illustrates the significant increase in the installation of wind and solar power around the world.

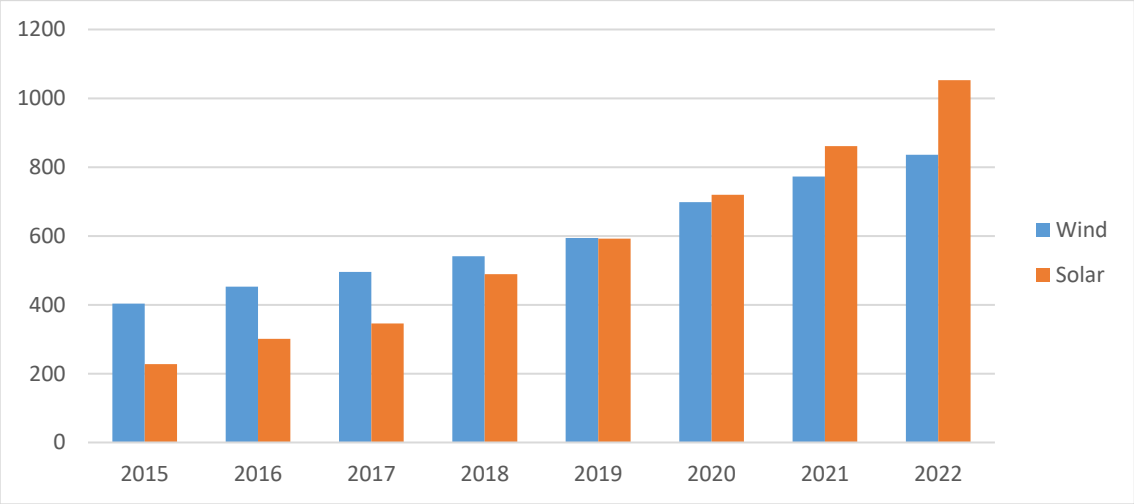

Figure 1. Global installed capacities of wind and solar power in GW (International Renewable Energy Agency, 2023; IEA, 2023).

The installation capacity of wind turbines increased from 403 GW to 836 GW, from 2015 to 2022 (IEA, 2023) , while the installation of solar energy increased from 228.92 GW to 1,053.12 GW, from 2015 to 2022 (International Renewable Energy Agency, 2023).

Renewable energy resources rely on natural patterns that vary depending on the surrounding weather conditions. For instance, the efficiency of solar energy varies according to the period of the day and whether the weather is cloudy or clear, which creates fluctuation and uncertainty that can cause grid instability (Zhang et al., 2023). Therefore, the challenge lies in controlling renewable energy sources (RES) before integrating them into the grid (Miyagi et al., 2015). As the scale of renewable energy installations increases, the variability in their output will eventually become one of the main factors affecting the reliability and resilience of the electric grid (Wenrui et al., 2022).

Grid codes were initially implemented more than twenty years ago. They are a set of regulations and standards that are utilized to regulate the operation of the grid to increase the flexibility, stability, and security of the electrical system (Flores & Loaeza, 2022a). Grid codes play a vital role in the process of integrating renewable energy resources into the grid by providing basic guidelines to ensure reliable grid operation. (Sarup et al., 2023).

Grid codes outline the basic capabilities and requirements for distributed energy resources connected into the grid. These codes help to maintain the stability of grid operation and have become essential as the renewable energy resources are increasingly integrated into the electrical grid system. Grid codes drive the shift towards a sustainable future by facilitating the integration of renewable energy into the grid. Therefore, the importance of grid codes increases as the amount of renewable energy resources integrated into the grid increases (Shanmugam et al., 2020).

The integration of renewable energy resources into distribution network is increasing substantially (Mahela et al., 2019). This global penetration of large-capacity renewable energy into the grid has raised substantial concerns regarding the stability of electrical grids. As a result, power grid operators have created corresponding standards and grid codes, which differ considerably based on the needs of each nation (Mahela et al., 2019). Grid codes evolve in response to ensure grid stability by integrating renewable energy resources into the grid (Letaief et al., 2023).

Standards and grid codes have been issued for both synchronous generators and inverter-based renewable energy resources. Updates to grid codes and standards have been developed in recent years due to the increased amount of inverter-based distributed energy resources in the power systems. The modifications have been made to add support to the power system, to increase the penetration of renewable energy connected to the inverter and optimize the extraction of the energy supply (Xu et al., 2021).

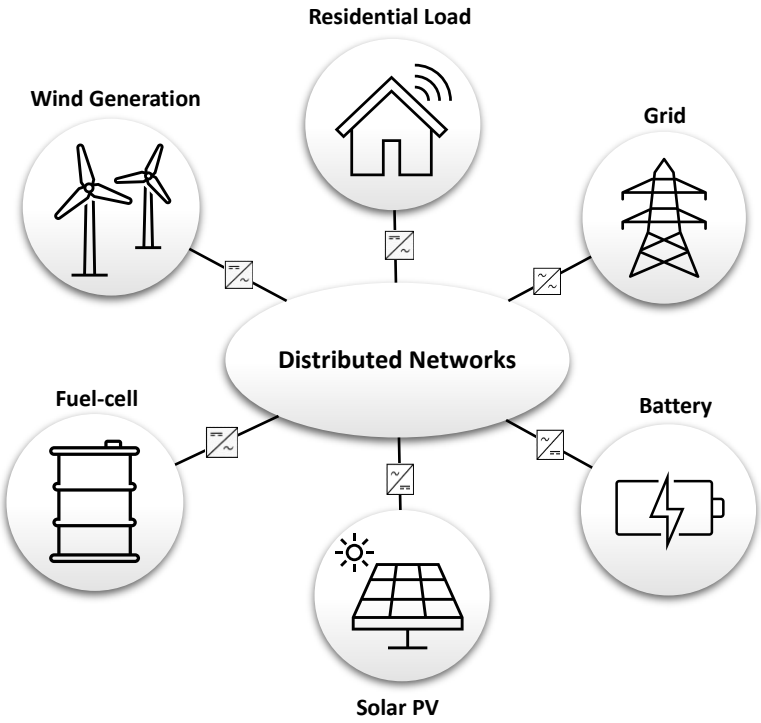

Figure 2. The typical structure of distributed network based on grid connected inverter (Hassan et al., 2024).

1.1 Motivation

The main challenge in integrating renewable energy resources into the grid is ensuring their compliance with grid codes. Therefore, it is crucial to test the compatibility of the renewable energy sources before integrating them into the grid, since they have a major influence that affects the overall reliability of the network. Therefore, grid code compliance testing is a mandatory process when integrating renewable energy resources into the grid to ensure the stability of the electrical system. Traditional on-site grid compliance type certification tests are resource and time-consuming and involve extensive planning, coordination, and significant financial resources. However, system operators need to conduct tests to verify their compliance with the grid code requirements (Etxegarai et al., 2014).

Simulation-based compliance offers a safe and efficient alternative method compared to the traditional on-site testing method, which is often time-consuming and costly. Additionally, simulation-based testing can emulate real-life scenarios, including grid conditions and fault situations, without the need for a direct connection to the actual grid, which also minimizes the risk of equipment damage during tests. Moreover, it also reduces costs for industrial manufacturers by accelerating the certification process, minimizing the costs required for the physical testing, and enhancing product reliability by allowing early detection and correction of potential compliance issues, leading to more efficient and effective certification process (Drechsler et al., 2022).

1.2 Objectives

This master thesis aims to develop a simulation process for testing grid code compliance using MATLAB Simulink. The purpose is to create a safe and efficient method for demonstrating compliance. The focus is on simulating different UVRT and OVRT scenarios for an inverter connected to the grid. Furthermore, the OPAL-RT real-time simulator will be utilized to execute the model in real-time software-in-the-loop. The thesis will comply

with EN 50549-1, EN 50549-2, and EN 50549-10 standards. The first two standards define the necessary functions, and the third standard provides instructions on how to conduct the tests.

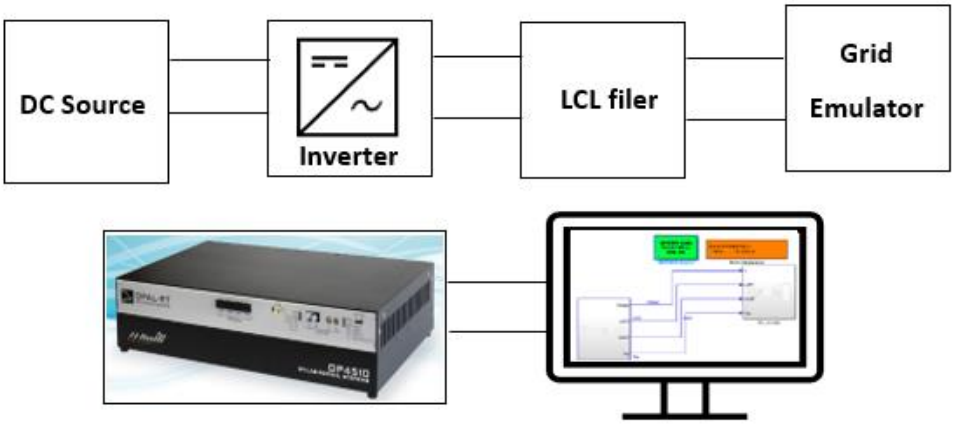

Figure 3. A general overview of the thesis objectives.

The objective of the thesis is to develop two comprehensive simulation models to test the capability of the generating modules to withstand voltage and frequency disturbances. The first model will focus on UVRT and OVRT; it will utilize relational operators to compare signals during events with pre-set thresholds. The UVRT and OVRT curves will be divided into three zones, and a minimum of two tests will be conducted in each zone to evaluate the simulation model. Additionally, a voltage-frequency block will be developed to enable continuous monitoring of the entire system, which will allow for observation of the voltage and frequency fluctuations from normal operation throughout the entire run time of the simulation.

The second simulation model aims to assess the response of the generating modules to over-frequency and under-frequency events. This model will utilize a frequency relay, a programmable voltage source, and a circuit breaker to simulate various grid disturbances. The aim is to evaluate the efficiency of the response mechanisms, such as activating the circuit breaker to isolate the grid, to ensure safe and reliable operation.

1.3 Related work

According to Magnago et al. (2021) , modern grid codes have been developed to be suitable for distributed energy resources and microgrids. The study provides a detailed investigation of the hardware-in-the-loop (HIL) test method. An overview of successful industrial cases utilizing HIL technology for certification and pre-certification is provided. These industrial cases are used for evaluating the compliance and performance of electrical inverters connected to solar energy and other electronic devices. The advantages and challenges of conducting grid code testing using the HIL technology method were also highlighted in their study.

Hafezi et al. (2021) highlight the challenge of full-power grid code compliance testing, which is time and resource consuming. Therefore, they developed an alternative simulation model based on a full-power laboratory test bench that is capable of testing the inverter's compliance with grid codes. They verified the accuracy of the model by comparing the simulated results with the experimental outcomes. The comparison showed that the simulation model reflected the dynamics of the experimental setup, especially in representing the performance of the inverter during fault ride-through (FRT) tests.

The laboratory test setup and the device under test in Hafezi et al. (2021) were simulated using Simscape toolboxes from MATLAB Simulink. The inverter was implemented based on average modeling, and it showed good dynamic behavior. They were able to evaluate the dynamic behavior of the inverter by using a simplified simulation model while testing the fault ride through. The simulation model proposed was simplified by replacing the experimental DC-DC converter with an ideal voltage source in the simulation model and ignoring its effect on the dynamics of the DC bus voltage during fault ride-through testing to ensure that the model is accurate, simple, and fast enough to test inverter-based grid compliance, which is necessary for adoption by grid operators.

Rafiq et al. (2022) employ a frequency domain method in their study to analyze stability and accuracy in power-hardware-in-the-loop (P-HIL) testing for UVRT of inverter-based renewable energy resources connected to the grid under both symmetrical and asymmetrical line-to-line fault conditions. The testing process involves creating realistic conditions and scenarios to assess power electronics converters by emulating the grid in real-time. To evaluate the accuracy of the experimental and P-HIL results, they were compared with the simulation test results using MATLAB/Simulink.

Zhang et al. (2016) describe a flexible hardware-in-the-loop test platform for evaluating grid codes, with a particular focus on UVRT capabilities. The platform was employed to assess the performance of solar inverters under fault conditions. It employed Field-Programmable Gate Array technology (FPGA) to emulate inverters connected to solar PV systems. An automated computing engine named Electrical Hardware Solution (eHS), developed by OPAL-RT, enabled the modification of the simulated circuit on the FPGA using commonly used simulation tools such as SimPowerSystem in MATLAB or PSIM.

Moreover, RT-LAB and eFPGAsim software packages were utilized to perform real-time simulations on both CPUs and FPGAs. The configuration of this platform can be easily modified without requiring FPGA programming knowledge for implementing UVRT tests. To validate the accuracy of their results, they compared the offline simulation with the real-time simulation results.

The primary aim of Stockl et al. (2018) was to utilize Controller Hardware-in-the-Loop (C-HIL) method for conducting a pre-evaluation technique of smart grid systems using Typhoon HIL 602 and interprocessor communication (IPC). This approach aimed to evaluate the power system's compliance to the grid codes during the design phase, prior to full implementation to reduce time to market by detecting errors early.

The HIL setup included Digital Signal Processing (DSP) and FPGA integration with current and voltage control, as well as a server protocol to evaluate grid code compliance. Four

grid code compliance testing cases for inverter-based systems were presented. One of these tests evaluated UVRT compliance with a 20% voltage dip. This test did not involve communication with the high-level manager; the UVRT zones such as "must remain connected" and "must disconnect" were programmed before the experiment. To verify the accuracy of the C-HIL tests, the results were compared with the laboratory tests.

Menegazzo et al. (2021) present a study on pre-certification of an automated test methodology for UVRT of a three-phase or single-phase PV inverter, as well as potential faults that may arise from the inverter using HIL and Python scripts. The aim of this study is to support the development of PV inverters by investigating their real behavior and providing reliable results. UVRT tests were conducted using a C-HIL real-time simulation. The experimental results for the grid compliance testing process of the UVRT test were presented to verify the pre-certification methodology.

Nithya & Roselyn (2022) proposed a control method for a multi-mode inverter, which refers to an inverter capable of operating in multiple modes or configurations, to enable fault ride-through capability while complying with grid codes. The study focuses on situations such as grid faults, grid stability, and the inverter's response to grid code compliance requirements. This strategy was implemented using MATLAB Simulink 2018b environment to conduct UVRT and OVRT tests to assess compliance with grid codes. The performance of the proposed control strategy was evaluated through hardware experiments with a grid-connected solar PV system.

Table 1 presents a summary of the previous studies with similar objectives to this master’s thesis, which have been highlighted in this section. These studies specifically focused on real-time or online simulation techniques for compliance testing of various grid codes.

Table 1. Comparison between different research papers.

Ref.	Tests	Simulation	Methodology	Comparison
Magnago et al. (2021)	UVRT-Freq	Real-Time	C-HIL	C-HIL and laboratory tests
Hafezi et al. (2021)	FRT	Simulink	Lab test	laboratory and simulation
Rafiq et al. (2022):	UVRT	Real-Time	P-HIL	P-HIL and Simulink
Zhang et al. (2016)	UVRT	Real-Time	HIL	HIL and offline simulation
Stockl et al. (2018)	UVRT-Freq	Real-Time	C-HIL	C-HIL and laboratory
Menegazzo et al. (2021)	UVRT	Real-Time	C-HIL	C-HIL and expected results
Nithya & Roselyn, (2022)	UVRT-OVRT	Simulink	Lab test	experiment and simulation

1.4 Thesis structure

This thesis comprises six main chapters. Beginning with defining grid codes and introducing modern grid code requirements. The next chapter provides the data and operating parameters for the simulation model based on EN50549-1 and EN50549-2 standards, including UVRT and OVRT thresholds and acceptable frequency deviations. The subsequent chapter outlines the methodology for modeling and controlling the grid-tied inverter using MATLAB Simulink. The next chapter introduces the main simulation model to develop a grid emulator for grid codes compliance during overvoltage, undervoltage, over-frequency, and under-frequency scenarios. The concluding chapter presents the results and discussion of the simulation model, providing insights into the inverter's performance and compliance with grid codes.

2 Grid codes and fault ride through requirements

Grid codes define the technical and operational characteristics of electrical systems. These codes vary between countries globally and also depend on specific processes required within the electrical system. However, there are several common technical specifications designed to ensure a high quality of energy supply from generation, distribution, and transmission to end users (Flores & Loaeza, 2022b).

Grid codes can be defined as a comprehensive technical document that includes all aspects of the electrical system, from operation to development and maintenance. Each grid code contains several regulations and guidelines to control the electrical system. These guidelines are a set of rules designed to enhance the reliability and stability of the energy supply (Flores & Loaeza, 2022b).

The key parameters of grid codes, including voltage, current, active, and reactive power, are essential measurement factors for controlling and determining the integration of renewable energy into the grid. Conducting several stringent tests is necessary to ensure that the RES meets the standards before integration. Modern grid codes, such as voltage stability, fault location, and fault ride-through, are examples of the continuous evolution of grid code requirements over time. Figure 4 depicts some basic requirements for obtaining modern grid codes (Sathiyanarayanan & Vijay M., 2024).

Grid codes are established by transmission system operators (TSO) to ensure reliable integration of power sources into the national electricity grid. In Finland, Fingrid serves as the sole TSO, supervising the entire national grid. In some countries, there are multiple TSOs responsible for managing the entire national grid. For instance, Germany has four TSOs: TransnetBW, Amprion, TenneT, and 50-Hertz Transmission. Each TSO is responsible for a specific area or sector of the national network. (Laine, 2020).

Grid codes have evolved to meet the modern requirements of the electrical network. Voltage control, frequency control, fault ride-through, active power control, and reactive power control are some of the essential grid code requirements (Padmanaban et al., 2023).

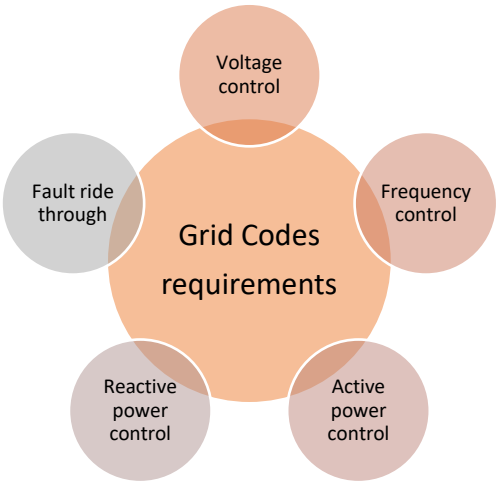

Figure 4. Essential grid code requirements.

Fault ride-through is the ability of renewable energy resources to remain connected to the grid and to provide support during electrical disturbances (Hadjidemetriou et al., 2015). The requirements to test the tolerance of grid voltage deviations are called under-voltage ride-through tests (UVRT) and over-voltage ride-through (OVRT) tests. (Laine, 2020).

2.1 Under voltage ride-through

The grid voltage maintains a nominal operating point, allowing the power generating modules (PGU) to continue operating without interruption. However, the power generation units must be able to remain connected during short periods of voltage deviation to avoid the occurrence of successive outages in the network when a slight decrease in voltage occurs (Laine, 2020).

UVRT capability refers to the ability of the generating modules to remain connected during a fault, resulting in a low voltage condition on a distributed system (Haupala & Bhumkittipich, 2019).

Utilizing solar photovoltaic (PV) and wind turbines encounters challenges during faults, which can result in voltage dips. These dips may occur due to various reasons, since renewable energy resources are dependent on weather conditions. Sudden changes, such as clouds affecting solar panels or changes in wind velocity impacting the turbines, may lead to disconnection from the power grid, causing power outages and instability. Therefore, to reduce these risks and ensure continuous operation of the grid, solar and wind systems must have UVRT capability.

For solar systems, UVRT capability is an essential requirement for inverter-based distributed energy resources. It determines whether the solar panels can remain connected to the grid during temporary voltage fluctuations (Cui et al., 2022). Wind turbines are also vulnerable to sudden voltage drops due to faults. Therefore, by having sufficient UVRT capability, wind turbines can remain connected to the grid during voltage sags. This contributes to maintaining grid stability and enables the continuous generation of power by wind turbines. Therefore, UVRT is one of the basic requirements set by TSOs when integrating wind turbines into the grid (Niu et al., 2018) . It enhances the stability of the grid connected to wind turbines, provides the ability to handle voltage drop situations, and increases the network's ability to provide reactive power support to maintain the voltage of the grid during faults (Akanto et al., 2021).

Figure 5 provides a representation of the UVRT voltage-time curve. Area A represents the nominal operating point where the generation units can continue to operate without dynamic support. Area B defines the period during which generating units must continue operating and supply reactive power support for a short period until the voltage recovers to the nominal operating conditions. Area C defines the situation where generating units are allowed to disconnect from the

grid (Laine, 2020). The UVRT curve depicted in Figure 5 was generated by a MATLAB script and inspired by the EN50549-1 standard.

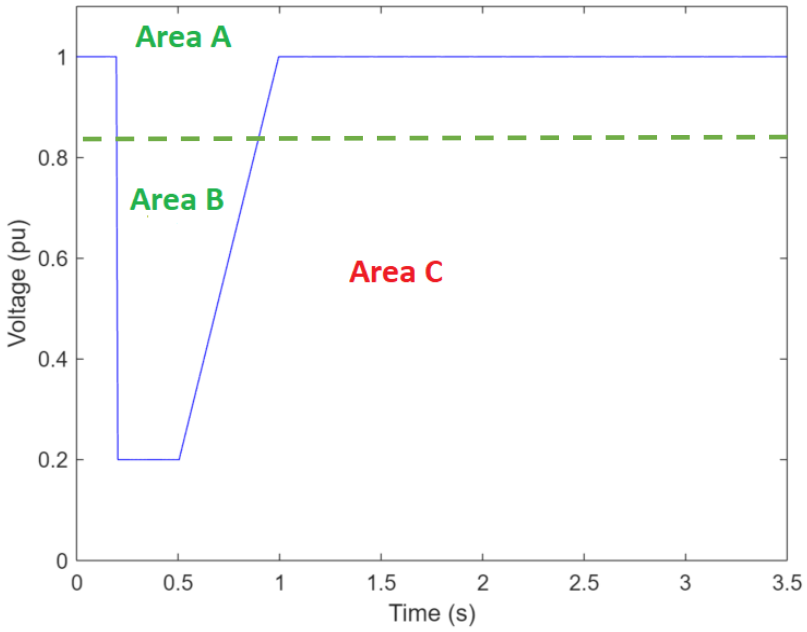

Figure 5. Under-voltage ride-through curve.

2.2 Under-voltage ride-through test setup

The test setup outlined in the EN50549-10 standard provides a framework for conducting realistic UVRT test events to emulate grid dips. This refers to situations when the voltage in the electrical system decreases from the normal level for a short duration. This can happen due to various reasons, such as short circuits or sudden changes in demand. An undervoltage event is achieved by a short circuit emulator capable of generating both three- or two-phase low voltage events to conduct a UVRT test, as depicted in Figure 6. Undervoltage event is generated by connecting the switch S_2 to the impedance Z_2. The decided voltage level for the test can be achieved by choosing the size of the impedance Z_2. The switch S_2 must have the capability to precisely control the between the connection and disconnection time.

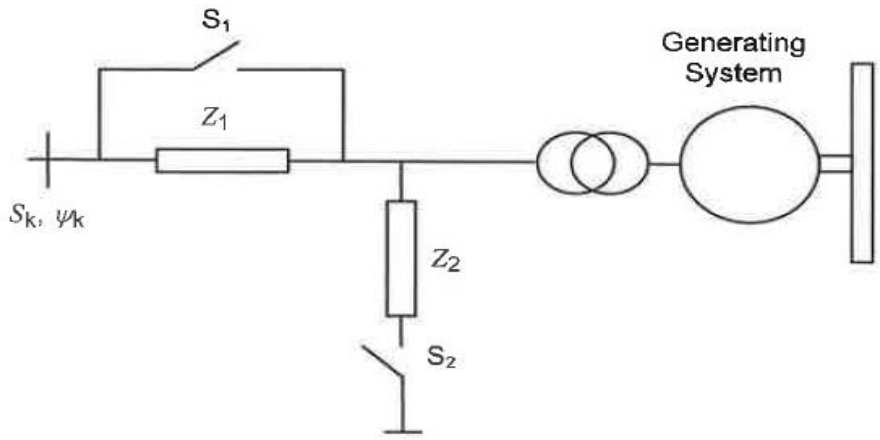

Figure 6. Under voltage ride-through test setup (Finnish Standardization Association SFS ry, 2022)

Z_1 is utilized to protect the grid by reducing the effect of the short circuit. The size of the impedance can be adjusted to ensure that the under-voltage event testing does not cause unacceptable conditions at the upstream grid and to minimize the impact on the transient response of the generating system. The operation of the by-pass switch S_1 can be applied before or after the voltage drop is performed. However, the operating time of the bypass switch should be recorded to avoid interference with the test.

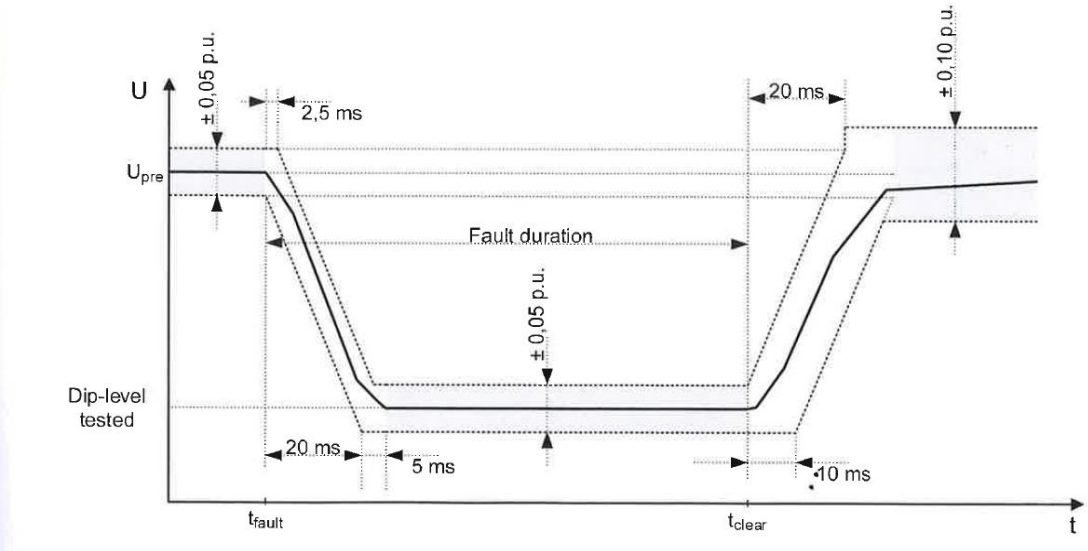

Figure 7. Tolerance of positive sequence voltage for undervoltage (Finnish Standardization Association SFS ry, 2022).

To enhance the clarity of the information presented in Figure 7, it is necessary to clarify the terminology used. Firstly, U_{pre} signifies the voltage value just before the under-voltage event occurs. Dip-level tested refers to the level of voltage drop experienced during the event. t_{fault} refers to the moment at which a short circuit occurs, which indicates the start of the under-voltage event. Finally, t_{clear} indicates the start of the voltage recovery to normal levels or the opening of the short circuit switch, respectively (SFS-EN 50549-10, 2022).

In the case of testing a specific generator, it is essential to disconnect other generating systems, such as wind turbines or solar panels, from the grid. The operation of these systems can affect the voltage required for the test. The voltage-time characteristics for the voltage dip events without the connection of the generating system are indicated in Figure 7. Measuring the voltage dip should be done on the voltage waveform at the output terminals of the test equipment. In addition, the test equipment includes time tolerance, which allows minor timing variations. It ensures that the calculated positive sequence voltage will not rise or fall except with a slope of one line period for the RMS calculation (SFS-EN 50549-10, 2022).

2.3 Over voltage ride-through

Over-voltage ride-through refers to the ability of the generating modules to remain connected for a short period of time when the voltage increases slightly above the nominal voltage. The voltage-time curve depicted in Figure 8 was generated using a MATLAB script based on the EN50549-1 standard. Region A represents the nominal operating condition, where the generating module should be capable of remaining connected without dynamic support. Region B indicates the acceptable overvoltage stage, where the voltage rise is below the OVRT threshold. The generating modules should remain connected and support reactive power injection to provide dynamic support and mitigate grid voltage. Region C represents the stage where the generating modules may disconnect from the grid as the voltage rise exceeds the OVRT threshold (Laine, 2020).

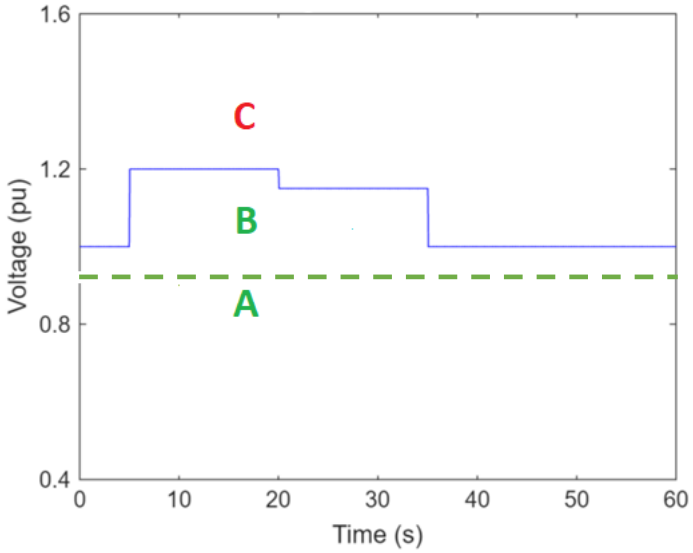

Figure 8. Over-voltage ride-through curve.

While OVRT is less common compared to UVRT, it still remains a requirement in most grid codes (Laine, 2020). A short duration of voltage swell is observed in utility grids. In response to such fluctuations, protection relays serve a critical function. These relays are connected to the inverter that interfaces with the grid. They monitor the function of the voltage and activate it to disconnect the inverter from the grid during unacceptable voltage swell conditions (Lone et al., 2023).

Z. Li et al. (2019) analyzed three distinct topologies of OVRT testing mechanisms to evaluate the OVRT capabilities of the PV connected to the inverter. This study focused on the components of various tests and suggested a principle for simulating different OVRT scenarios. It provides suggestions for both laboratory and on-site tests.

2.4 Over voltage ride-through test setup

The test setup of OVRT is utilized to emulate over-voltage grid scenarios such as the Ferranti effect. This occurs when the voltage at the receiving end of the transmission line is higher than the voltage at the sending source (Foqha et al., 2023).

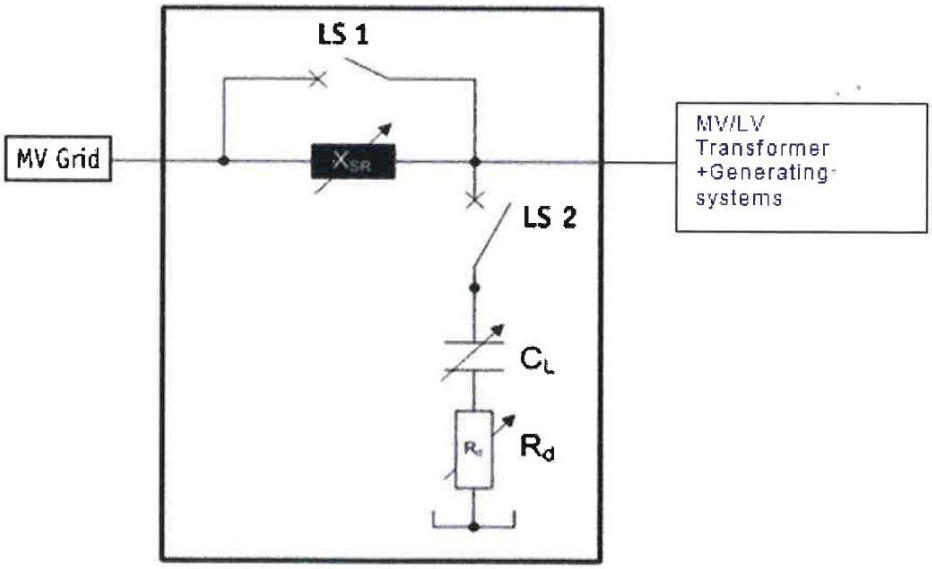

Figure 9. Capacitor based OVRT test setup (Finnish Standardization Association SFS ry, 2022).

A realistic OVRT test setup is outlined in EN50549-10. As depicted in Figure 9, this methodology employs a capacitor, impedance, and circuit breakers. The over-voltage event is initiated by connecting the impedance, consisting of a capacitor C_L and R_d through the breaker LS2. The values of C_L and R_d are adjustable to match the specified voltage magnitudes required for conducting the test. This test setup enables accurate emulation of over-voltage grid scenarios, such as the Ferranti effect.

The impact of the test sequence on the up-steam grid is limited to the impedance X_{SR}. The size of this impedance can vary depending on the test requirements, while ensuring that the selected size does not lead to unacceptable situations for the upstream grid or significantly affect the transient response of the generating systems.

Connecting X_{SR} (LS1) can occur prior and after the voltage rise that is initiated by operating LS2 (SFS-EN 50549-10, 2022).

In the initiation of testing a specific generator, it is crucial to disconnect all other generating modules, such as wind turbines or solar panels, to ensure that the voltage required for the test remains unaffected by other generating systems. Circuit breakers LS1 and LS2 can be mechanical circuit breakers or other devices and should be selected based on their accuracy to control the duration of the voltage increase. The voltage-time characteristics for the voltage swell events are indicated in Figure 10.

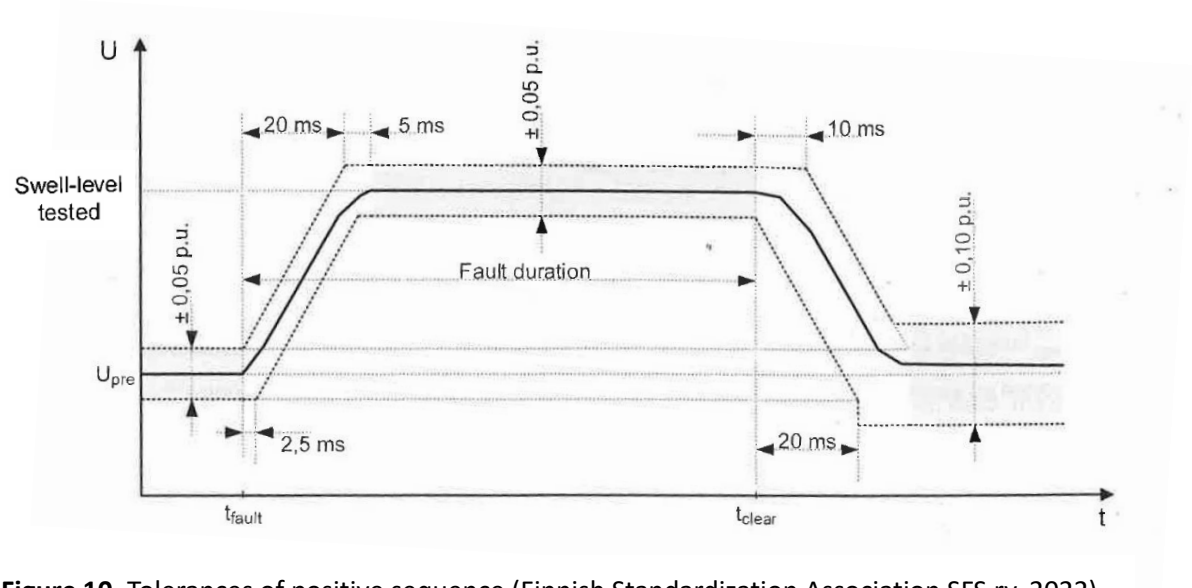

Figure 10. Tolerances of positive sequence (Finnish Standardization Association SFS ry, 2022).

U_{pre} in Figure 10 refers to the voltage value just before the under-voltage event occurs. Swell-level tested refers to the level of effort during the occurrence of the event. t_{fault} refers to the moment of a short circuit, which indicates the start of the event. t_{clear} indicates the start of the voltage recovery or the opening of the short circuit switch, respectively (SFS-EN 50549-10, 2022).

The specified capacity as a default requirement of generating modules of a synchronous generating technology from EN 50549-10 is illustrated in Figure 11.

The under-voltage capability (UVRC) and the over-voltage (OVRC) capacity are calculated as follows:

$$U_{UVRC} = U_n - U_{min}$$
$$U_{OVRC} = U_{max} - U_n \quad (1)$$

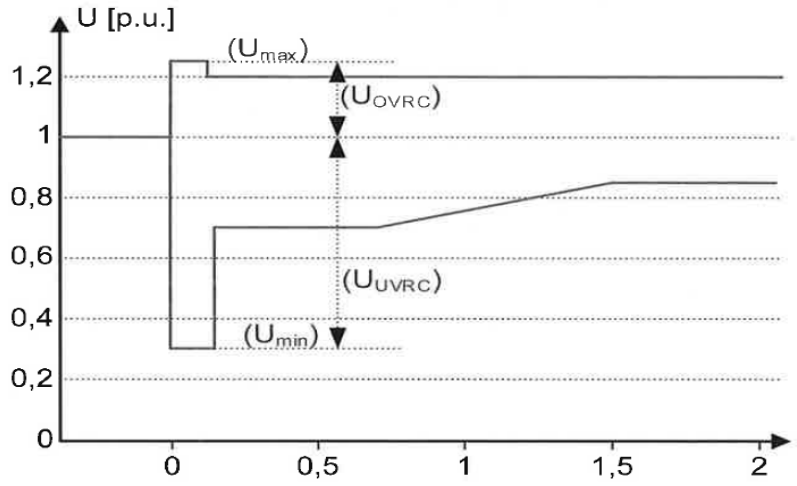

Figure 11. UVRC and OVRC default requirements (Finnish Standardization Association SFS ry, 2022)

Tests should indicate the maximum capacity of the generating units to withstand undervoltage and over-voltage events by selecting the longest duration of the dips and swells to prove the conformity of the generating units.

2.5 Frequency control

Frequency is an essential element that must be controlled to ensure the safe operation of the electrical system. It refers to the number of periodic events per second in an oscillating voltage electrical system and is measured in hertz. While the nominal frequency of the Nordic power system is set to operate at 50 Hz, the actual frequency continually oscillates around the nominal value. Consequently, it is critical for transmission system operators (TSOs) to restrict the frequency deviations of a power system to guarantee the quality and stability of the electrical system. In the event of a large frequency deviation,

the PGU cannot continue operating and will be disconnected from the grid (Modig et al. 2022).

Frequency is constantly subject to variation based on the imbalance between supply and demand. When electricity production exceeds consumption, the frequency increases, and conversely, it decreases when consumption exceeds production. These frequency fluctuations are mitigated by the kinetic energy, or inertia of the system. In the Nordic region, most of the power plants utilize synchronous generators, whose rotor's rotational speed determines the frequency. The system's kinetic energy is derived from synchronously connected masses, including generators and turbines (Modig et al. 2022).

Modig et al., (2022) described three fundamental elements for determining frequency in the electrical system:

(1) Power imbalance refers to an imbalance between production and consumption. A large imbalance can occur by disconnecting a large production unit, which will generate a larger frequency deviation.
(2) Kinetic energy refers to the accumulated rotational energy in all the machines that are synchronously connected. Increased kinetic energy results in a higher rotational mass to reduce the change in frequency caused by the imbalanced power.
(3) Reserves from PGU: consumption units and energy storage units that control the amount of energy exchanged with the grid to ensure the balance of the power system.

2.5.1 Frequency disturbance

Ride-through tests are utilized to test the frequency disturbance of a system. Tests are conducted to verify the behavior of the system under abnormal frequency conditions to ensure grid frequency stability. The grid codes specify the range of frequencies where

the network can continue to operate normally, as well as the permissible levels for temporary disturbance frequencies and the instantaneous trip level (Laine, 2020).

Ahmed et al. (2023) study included a comprehensive review of the role of grid codes and standards to ensure dynamic grid stability when integrating inverter-based renewable energy resources. To achieve a balanced power distribution between generation and consumption, the system regulates the frequency within pre-determined operational boundaries, which are close to the nominal operating frequency. When demand surpasses generation, the frequency serves as an equilibrium parameter between generation and demand. In the event of unexpected disturbances, the rotating masses of the grid-connected synchronous generators will respond to the frequency dip situation by providing a natural inertia reaction.

When the speed of the rotating machine as well as the frequency in the system are reduced, it provides enough time to allow the governor-equipped synchronous generators to prevent any frequency fluctuations during the initial phases of the disturbance, which is called the primary frequency response. As a result, the secondary frequency response restores the system to stability and returns the frequency to normal operation (Ahmed et al., 2023). Figure 12, generated using MATLAB Simulink, illustrates the fundamental stages of the frequency control mechanisms in a conventional power system following a significant disturbance.

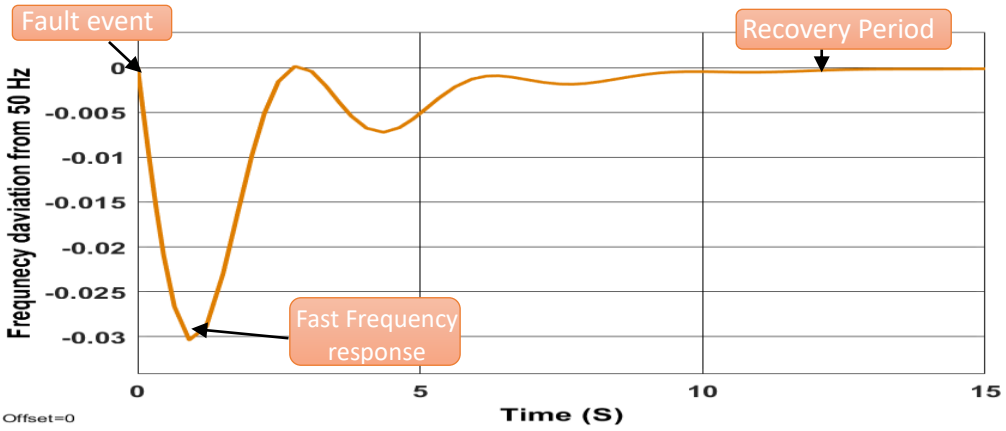

Figure 12. Frequency control mechanism following generation loss.

2.5.2 Rate of change of frequency

Rate of change of frequency (ROCOF) refers to the capability of modules within a power generation plant to maintain the connection to the distribution network and operate when the frequency of the distribution grid fluctuates within the defined threshold. ROCOF plays a pivotal role in assessing the stability of grid immunity, especially with the increasing amount of distributed generation (DR). It is used to control the systems, regulate power balance, and provide system inertia for the electrical grid (Rietveld et al., 2020). ROCOF is considered the primary indicator to detect the occurrence of a fault in the network. Consequently, it is used in some countries to detect if the power plant has lost connection with the main grid. Moreover, isolated or small distribution networks, such as islands, require greater immunity values for the ROCOF to enable immunity against faults (SFS-EN 50549-2, 2019).

Interface protection settings are responsible for detecting and responding to changes in the electrical system. They depend on two key factors: the technical capability and the connection setting of the interface. Technical capability refers to the capacity of the system to perform a function or withstand a certain condition, while connection setting determines when the generating plants should be disconnected from the grid. Frequency relays are commonly used in interface protection systems. They can be utilized for monitoring and controlling the frequency. These relays can be configured by setting their value to monitor either ROFOC or over-frequency and under-frequency situations (Albu et al., 2014).

According to the EN50549-2 standard, immunity to ROCOF is defined by a sliding measurement window of 500 milliseconds. All generating modules and components within the generating plant that could potentially lead to their shutdown must have the same level of immunity. It should meet or exceed the specified threshold determined by the responsible authority.
If the ROCOF immunity is not defined, the ROCOF will be determined based on the generating technologies as follows:

(1) The minimum ROCOF for non-synchronous generating technology is 2 Hz per second.

The minimum ROCOF for synchronous generating technology is 1 Hz per second.

EN50549-10 provides verification procedures for ROCOF, over-frequency, and under-frequency conditions using a grid emulator capable of controlling the frequency within the required dynamic range for the test. The initial condition of the generating unit for conducting the test should be as follows: the grid emulator should operate within the range of 100% to 80%. Additionally, maintain an active factor equal to 1, and the ROCOF protection functions should be deactivated during the test.

The test should be performed as per the sequence represented in Figure 13. To evaluate the ROCOF, the grid emulator will adjust the frequency at the generating terminals to create over-frequency and under-frequency conditions, according to the specifications detailed in Table 2. Moreover, the frequency modulation by the grid emulator should be linear over time, which means that the change in frequency should occur at a constant rate. The grid emulator will verify the reaction of the generating module under both over-frequency and under-frequency conditions.

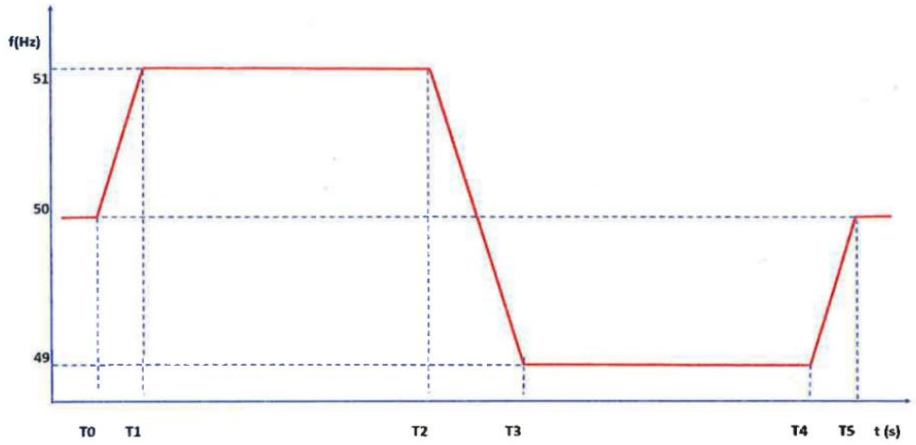

Figure 13. ROCOF test (Finnish Standardization Association SFS ry, 2022)

During these verifications, once the high or low threshold is reached, it should remain at that point for at least 3 seconds. This duration is the required time for the system to stabilize during a real event (SFS-EN 50549-10, 2022).

Table 2. Frequency steps during Rocof (Finnish Standardization Association SFS ry, 2022).

Step	**Frequency**	**ROCOF / time**
T0	50Hz	-
T0 to T1	-	=Required ROCOF Value
T1 = T0 + (Required Minimum Measurement Time)	50 Hz + (Required ROCOF Value) x (Required Minimum Measurement Time)	-
T1 to T2	-	Zero
T2 = T0 + (Required Minimum Measurement Time) + 3s	50 Hz + (Required ROCOF Value) x (Required Minimum Measurement Time)	-
T2 to T3	-	=Required ROCOF Value
T3 = T0 + 3 ×(Required Minimum Measurement Time) +3s	50 Hz – (Required ROCOF Value) x (Required Minimum Measurement Time)	-
T3 to T4	-	Zero
T4 = T0 + 3 ×(Required Minimum Measurement Time) +6s	50 Hz – (Required ROCOF Value) x (Required Minimum Measurement Time)	-
T4 to T5	-	=Required ROCOF Value
T5 = T0 + 4 ×(Required Minimum Measurement Time) +6s	50 Hz	-

2.6 Active power response to frequency

Frequency is an essential index for all characteristics of the electrical system, as variations in the frequency range reflect changes in the active power (C. Li et al., 2020). Therefore, active power control is required to produce an amount of energy specified by the DSO, or responsible party, to maintain the stability and reliability of the electrical grid. PGU must be capable of maintaining the active power as per the target value, even during frequency fluctuations, unless the frequency code mode is active. Frequency code mode involves modifying the power output of the generating modules in response to changes in frequency, to control the frequency deviation within a predefined threshold (Fingrid, 2018).

2.6.1 Active power response to over-frequency

The reliability of the system depends on maintaining a balance between active power and load demand, to maintain the nominal operating frequency. Active power response to over-frequency, also known as frequency control or Limited Frequency Sensitive Mode–Over-frequency, refers to the ability of the power generating modules to adjust the output power when the frequency of the grid exceeds the nominal condition. (SFS-EN 50549-1, 2019). When the power demand increases, all generators within the grid allow frequency to droop, which will help in balancing the load between all the generators on the grid. To help the frequency to maintain its nominal value.

Traditional electric power systems, such as those powered by fossil fuels, utilized speed regulators to control the frequency deviation of the electrical system during fault conditions. storages are equipped with control systems that include strategies such as frequency droop, to enhance the overall efficiency and provide grid support (G. Landera et al., 2023).

As per the EN50549-1 standard, the generating modules must be capable of activating the power response to over-frequency at a programmable frequency threshold within the range between 50.2 Hz and 52 Hz. Additionally, this must occur within a range of 2% to 12%. This represents a gradient of 100% to 16.7% P_{ref}/Hz, the gradient g defined by the following equation:

$$\mathrm{g}\left[\frac{P}{P_{ref}}Hz\right] = \frac{1}{S.f_n} \quad (2)$$

where g is the active power gradient or droop relative to the reference power. It represents the changes in the output power of the generating modules in response to frequency changes. S defines the acceptable range before activating the power response, and it is expressed as a percentage of the nominal frequency. P is the actual active power of the generating module, and P_{ref} is the reference power when the frequency reaches a predefined threshold (f_1).

The deactivation threshold frequency (f_{stop}) deactivates the power response to frequency deviation once the frequency returns within the acceptable threshold. It is set based on the requirements of the electrical system. Alternatively, the DSO or the responsible party may define an additional deactivation threshold, within the range of 50 Hz and f_1. Response to over-frequency must be fast, with a maximum step time of 30 seconds, unless another value is determined by the responsible party**.** Figure 14 depicts the active power response to over-frequency. The active power should start responding to the over-frequency event once the frequency reaches the value f1. The programmable frequency threshold is set at f1 = 50.2 Hz, the programmable droop is set at 5%, and f_{stop} is deactivated in this case (SFS-EN 50549-1, 2019).

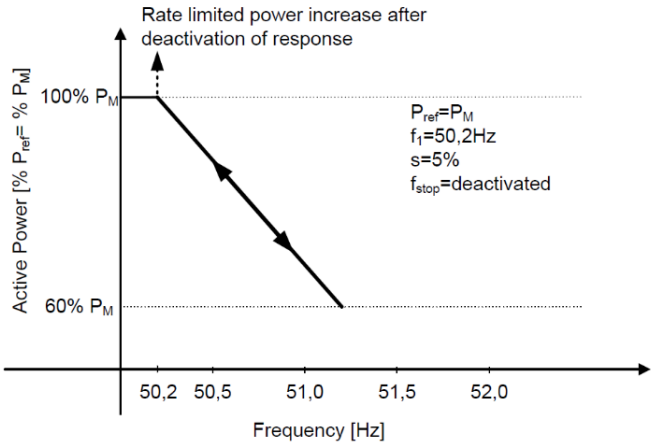

Figure 14. Active power response to over-frequency (Finnish Standardization Association SFS ry, 2022).

2.6.2 Active power response to under-frequency

Based on EN50549-1 and EN50549-2 standards, a generating plant unit must be able to withstand the frequency drop at the point of connection (POC) while minimizing the reduction of active power to a minimum extent. The solid line in Figure 15 illustrates the allowable decrease in active power due to a frequency decrease. The maximum permissible reduction rate is 10% of P_{max} per 1 Hz of frequencies below 49.5 Hz. In most stringent cases, the rate of active power decrease is 2% per 1 Hz at frequencies less than 49 Hz.

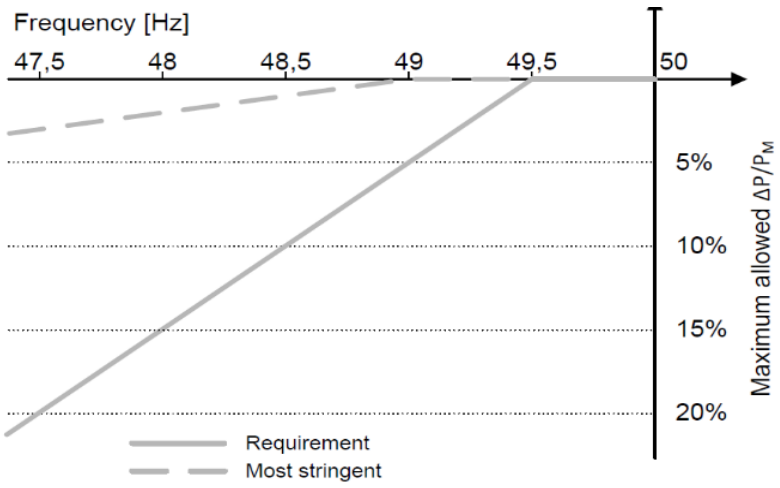

Figure 15. Underfrequency power reduction (Finnish Standardization Association SFS ry, 2022).

3 Simulation parameters

This chapter provides the data and operating parameters required to create the simulation model, based on EN50549-1 and EN50549-2 standards. It contains specific UVRT and OVRT thresholds, which specify the conditions under which the system must continue operating during voltage fluctuations. Furthermore, the chapter outlines the normal operating frequency ranges and the acceptable frequency deviations that the system can tolerate. The parameters outlined in the mentioned standards are essential for precisely simulating the behavior and efficiency of the generating modules under various conditions. This chapter establishes a solid basis for the subsequent analysis and simulation process in this thesis.

The standards were prepared by CLC/TC 8X (System aspects of electrical energy supply). This European standard covers the RFG European Network Code and the current technical market requirements. It provides a comprehensive explanation of the functions that need to be implemented in products, and it serves as a technical reference for national requirements. These specifications state the abilities and technical components of power plants that run with MV distribution networks. EN50549 includes all the capabilities necessary for generating plants to operate in parallel with distribution networks.

3.1 Normal operating range

Generating modules must have the ability to continue operating within the normal ranges defined by the electrical system, regardless of their structure or the protection breaker settings. To ensure that the generating modules can withstand typical fluctuations while maintaining the performance and stability of the electrical grid. The normal operating range includes nominal operating conditions and acceptable fluctuation ranges for the voltage and frequency that the generating modules must tolerate without activating protection interfaces or causing power interruption, which provides flexibility to ensure the integration of various power generation sources (SFS-EN 50549-1, 2019).

3.1.1 Frequency operating range

Based on the EN50549-1 standard, the generating plant should have the capability to operate when the frequency range at the POC is between 49 Hz and 51 Hz. In addition, the generating modules should have the capability to remain connected if the frequency in the operating zone occurs between 47 Hz and 52 Hz until the safety breaker is activated.

The generating modules in the system should operate within the strict limits outlined in Table 3. However, the DSOs or responsible parties can also request a longer duration or a broader range of frequencies. In such cases, their requests should be followed. As illustrated in Table 3, for the frequency ranges between 47.5 Hz and 48.5 Hz, the minimum required period of operation is 30 minutes, while the period for operation under stringent requirements is 90 minutes, etc.

Table 3. Frequency operation durations (SFS-EN 50549-1, 2019).

Frequency Range	Time period for operation Minimum requirement	Time period for operation stringent requirement
47.0 Hz – 47.5 Hz	not required	20 s
47.5 Hz – 48.5 Hz	30 min	90 min
48.5 Hz – 49.0 Hz	30 min	90 min
49.0 Hz – 51,0 Hz	Unlimited	Unlimited
51.0 Hz – 51.5 Hz	30 min	90 min
51.5 Hz – 52.0 Hz	not required	15 min

According to COMMISSION REGULATION (EU) 2016/631 Title 6. linear Stirling motors are a type of Stirling engine that utilizes a prime mover to produce a repetitive linear motion in a magnetic field, generating AC electric power. The AC electric power generated by them is classified as an emerging technology, granting them permission to

decouple at frequencies below 49.5 Hz and above 50.5 Hz. This permission does not affect the interface protection requirements. However, the over-frequency and under-frequency machine protection systems may trip before the interface protection system.

If the utilized technology or the ambient conditions impact power reduction within the system, the manufacturer must determine the suitable ambient conditions for the product applications, along with any other potential limitations. Information can be provided by the manufacturer through a graph that specifies the general behavior of the system under different ambient conditions. Therefore, the power reduction must comply with the ambient conditions previously provided by the responsible party. If the generating unit fails to meet the power reduction in the given environment, the producer and the responsible party must mutually agree on acceptable ambient conditions (SFS-EN 50549-1, 2019).

3.1.2 Continuous operating voltage range

The generating station must maintain a continuous connection during power generation operations, provided that the voltage at the connection point remains within the specified range of 85% to 110% of the nominal voltage U_n . Moreover, distribution networks are allowed to decrease to a level below 85% of the nominal voltage U_n for a temporary period. In this case, the manufacturers and operators must consider the operational capacity of the power plant. Voltages beyond those thresholds are considered the limits of immunity for under-voltage ride-through and over-voltage ride-through (SFS-EN 50549-1, 2019).

3.2 Immunity to disturbance

Immunity to disturbance refers to the capability of the generating modules to withstand disturbances and have the ability to remain connected. This section outlines the necessary immunity considerations for power plants, considering the requirements for connecting a generating unit in parallel with the grid. Additionally, it is also crucial to consider any additional components, such as transformers or tap changers, that might affect the generating plants (SFS-EN 50549-1, 2019).

3.2.1 Under voltage ride-through

Based on the EN50549-1 Standard, the generating plants must have the capability to remain connected to the grid as long as the voltage at the POC remains above the specified voltage-time curve. This curve illustrates the permissible voltage during short-term fault occurrences in the network. Figure 16 outlines the essential criteria necessary to maintain the connection between the generating plant and the grid. These criteria must be met, despite the settings of the interface protection.

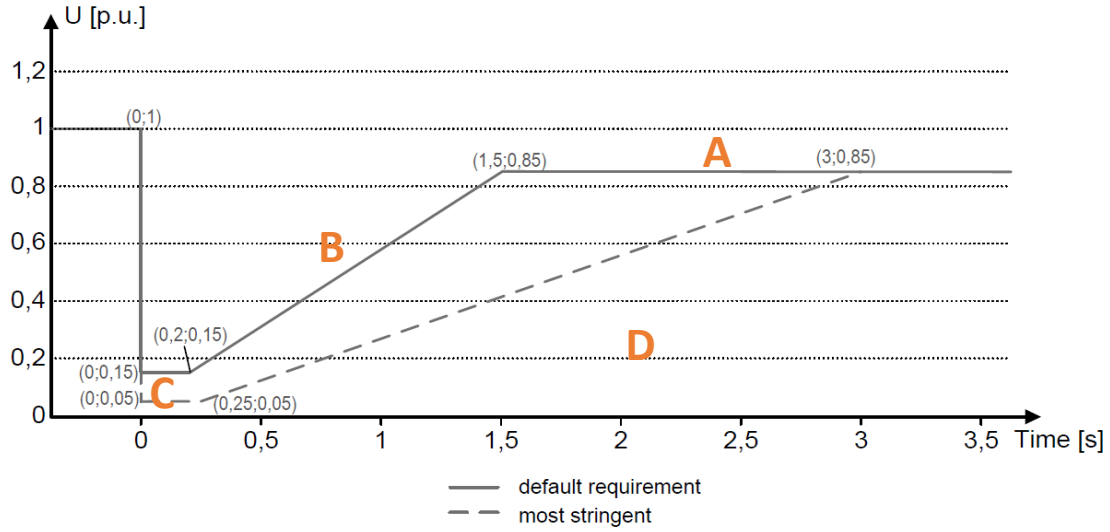

Figure 16. UVRT capability for asynchronous generating technology (SFS EN 50549-1, 2019).

The voltage-time curve defines the essential thresholds for meeting the UVRT requirements of a non-synchronous generation power plant based on the EN50549-1 standard. The responsible party has the authority to define different UVRT characteristics, which are expected to be similar to the more stringent curve in Figure 16. Moreover, the entire generating unit and the elements in the generating station that may cause their disconnection must comply with UVRT requirements. As illustrated in Figure 16, the curve was divided into four zones to facilitate the explanation.

Zone A represents the recovery phase, when the voltage starts to recover from the fault. The generating module must be capable of remaining connected to the grid with reactive power support. This zone represents the situation when a voltage recovers to 0.85 p.u. in less than 1.5 seconds following the occurrence of the fault. Moreover, it is essential for the generating modules to remain connected to the distributed generation during the recovery phase to ensure a stable function of the grid.

In Zone B, the generating modules must be capable of remaining connected to the distributed network with reactive power support. The maximum acceptable voltage drop thresholds are: 0.4 p.u. for less than 0.5 seconds; 0.6 p.u. for about 1; second and 0.8 p.u. for less than 1.5 seconds.

Zone C: When the fault occurs, the voltage may drop rapidly. Therefore, if the voltage drops briefly to a level above 0.15 p.u. for less than 0.2 seconds, the generating modules should have the capability to remain connected to the distributed network with the reactive power support.

Zone D: if a fault occurs and the voltage drops below the voltage-time curve. The generating modules should disconnect from the grid to maintain the stability and reliability of the grid. The disconnection of the grid is essential for the safety of the electrical system.

After the voltage returns to the continuous operating range, the generating modules must restore 90% of their pre-fault capacity. This must occur within a maximum period of one second, unless specified differently by the responsible party or the DSO. The entire generating plant, including all elements that may potentially cause interruption, must comply with the UVRT requirements. Generating units must remain connected to the distributed grid by ensuring that their terminals remain above the voltage-time threshold. The requirements are applicable to all types of faults, including single-phase, two-phase, and three-phase faults.

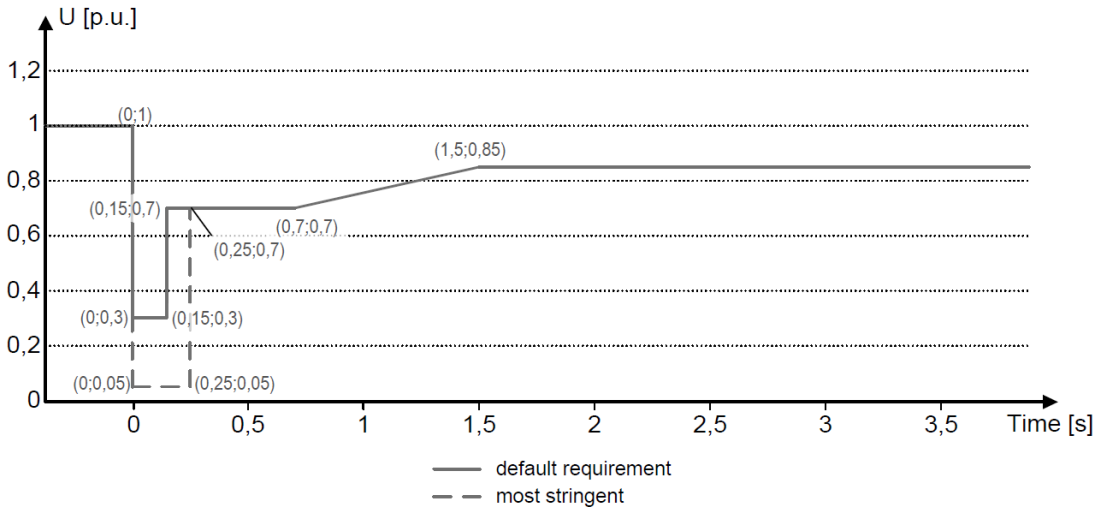

Figure 17. UVRT capability for synchronous generating technology (SFS EN 50549-1, 2019).

The same principle applies to synchronous generation technology. Generating modules must maintain their connection to the distribution network, provided that the voltage at the POC remains above the voltage-time curve depicted in Figure 17. It is essential to maintain the connection to the distribution network to ensure the stability of the electrical grid. The acceptable voltage thresholds during disturbances are defined by the voltage-time curve illustrated in Figure 17. Complying with this curve prevents potential equipment damage that can happen as a result of faults. To test the UVRT capability based on the EN50549-1 standard, the maximum phase-to-neutral, or if a neutral is not present, the maximum phase-to-phase voltage must be assessed.

3.2.2 Over-voltage ride-through

The generating modules, excluding micro-generating plants, must have the capability to remain connected to the grid when the voltage at the connection point remains below the voltage-time curve illustrated in Figure 18.

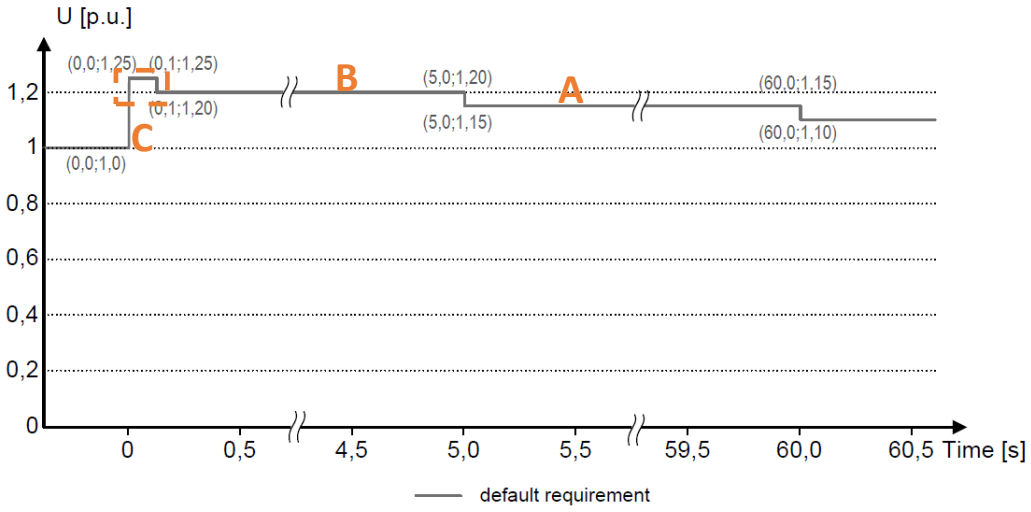

Figure 18. Over-voltage ride-through capability (SFS EN 50549-1, 2019).

OVRT capability illustrates the permissible voltage levels over a specific time interval to ensure the stability of the electricity supply. The curve begins at the nominal operation voltage of 1 p.u., under the condition that the generating modules must have the capability to continue operating normally. The rest of the curve can be specified into three main operating thresholds. These thresholds define different voltage levels that generating units must withstand to remain connected to the distributed generation:

Zone A: The first threshold in the voltage-time graph is 1.15 p.u. for less than 60 seconds. This means that if the voltage increases to a level below 1.15 p.u. and remains at this level for less than 60 seconds, the generating module must be capable of remaining connected. This threshold provides flexibility to the generating modules, by allowing them to withstand longer periods of elevated voltages without triggering disconnection.

Zone B: The second threshold is 1.20 p.u. for less than 5 seconds. This threshold includes a more severe, but shorter duration of voltage rises. If a voltage increases to a point less than 1.20 p.u. and remains for less than 5 seconds, the generating modules should be capable of remaining connected. This prevents unnecessary interruptions that may cause failures across the electrical grid, especially if faults happen frequently, leading to grid instability.

Zone C is a critical threshold in the electrical system that allows the voltage to increase to a point less than 1.25 p.u., for a duration of less than 0.1 seconds without causing disconnection. This means that if an over-voltage event occurs, and the voltage increases to less than 1.25 p.u. for less than 0.1 seconds, the generating modules should be capable of remaining connected, which contributes to the reliability and stability of the electrical network.

4 Modelling a grid-tied inverter

The main objective of this thesis is to develop a simulation model for grid code compliance testing using MATLAB Simulink. This chapter provides a foundation for the simulation model. Before conducting the tests, it is essential to model and control the grid-tried inverter. The chapter provides the methodology for implementing and controlling the inverter, utilizing MATLAB Simulink.

Electricity generation has historically been dominated by large power plants utilizing synchronous generators, which have the capability to produce reactive power. Their inherent large rotational inertia offers voltage support during short-term interruptions. They provide consistent and predictable primary energy production, which improves overall grid stability (Laine, 2020).

The shift towards utilizing inverter-based resources is growing significantly (Xu et al., 2021). Inverters facilitate the connection of renewable energy resources such as wind and solar into the grid by converting their direct (DC) current into alternating current (AC). The inverter must operate with high efficiency and be able to function in grid-connected or islanded mode (Istardi et al., 2017). Figure 19 illustrates the basic design of the DC-to-AC inverter.

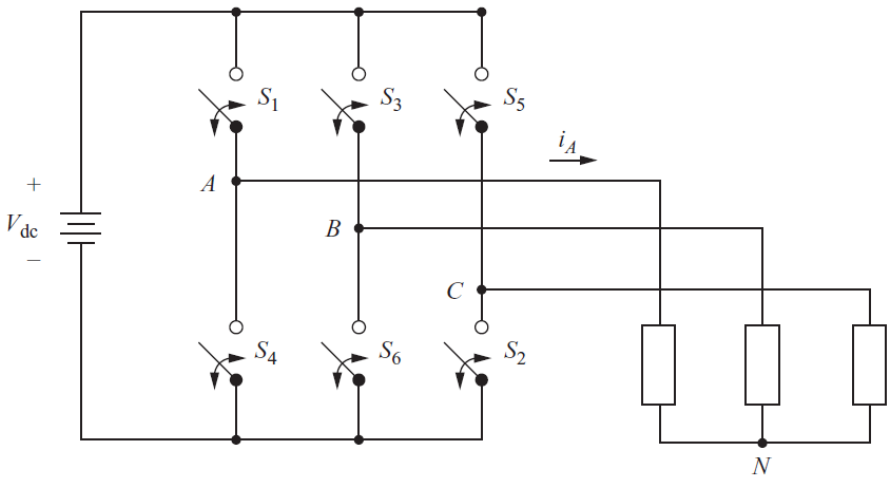

Figure 19. Three-phase inverter (W. Hart, 2010).

Inverters operate based on switching devices such as transistors, IGBTs, MOSFETs, or SCRs. Although the inverter converts DC current into AC current, the output power of the inverter will include harmonics, which reduce its quality (Istardi et al., 2017). Therefore, it is essential to incorporate filters to increase the efficiency of the system. Various filters can be employed, such as LC filters and LCL filters (Liu, 2016). High-frequency harmonics are reduced by connecting the inverter output to an LCL filter to ensure that the output power of the inverter aligns with the grid system (Istardi et al., 2017).

The inverter can produce different output signals, such as sine waves, rectified sine waves, or a square wave. Square-wave signals are utilized for low and medium power applications, while sine waves are common in high-power applications (Istardi et al., 2017). Power inverter circuits usually consist of two circuits, a power circuit and a control circuit. The power circuit consists of electronic power switches, filters, and other components that can vary based on the application. The components include a DC bus capacitor and a grid-side coupling transformer. The role of the control circuit is to monitor the operation of the inverter. (Hafezi et al., 2021).

4.1 Grid-tied inverter simulation

Figure 20 provides an overview of the model. A DC source in the simulation model represents renewable energy resources such as wind or solar panels. The inverter converts the DC current to grid-compatible AC power. An LCL filter is utilized to reduce the harmonics generated by the inverter output and increase the quality. The point of measurement is between the LCL filter and the grid. Figure 21 illustrates the power circuit and the PLL feedback control system of the grid tied inverter.

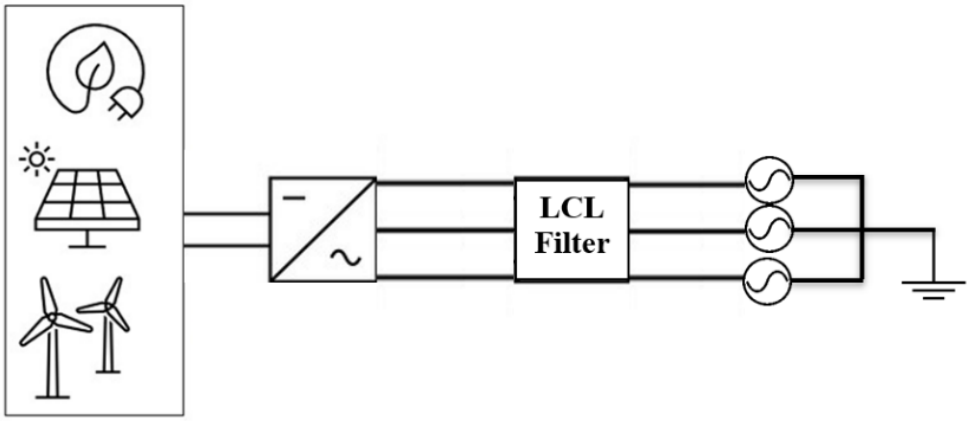

Figure 20. Grid-tied inverter connected to renewable energy resources.

V_{abc} represents the phase voltages a,b and c, respectively. abc to αβ block converts the three-phase signals into αβ stationary reference frame, which is simpler than the complex analysis of the three-phase systems, especially for controlling and regulating the inverter by reducing the variables into two orthogonal components α and β. Moreover, αβ to dq block transform αβ reference frame into dq rotating reference frame, which considered another essential step of power electronics systems and control, which simplify the analysis of the rotating machines and provides an effective control strategy. Furthermore, a PLL control system is implemented to synchronize the output waveforms of the inverter (Parvez et al., 2016).

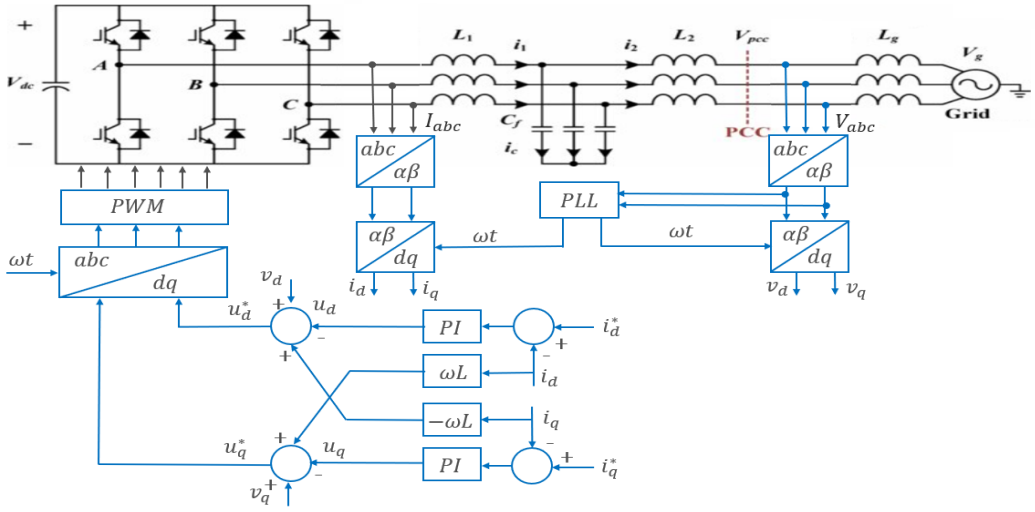

Figure 21. Inverter connected to the grid with PLL control circuit.

4.1.1 Control of inverters using αβ and dq transformations

Two reference frame approaches are employed to control the inverter: αβ and dq frame. This allows the use of the proportional controller (PI) controller to simplify the system while maintaining reliability. This method has been chosen because it is well-tested and widely used in the industrial sector (Roos, 2020).

The three-stage system can be represented mathematically as follows (Roos, 2020) :

$$\begin{aligned} f_a(t) &= \hat{f}\cos(\omega t + \theta_0), \\ f_b(t) &= \hat{f}\cos(\omega t + \theta_0 - \tfrac{2\pi}{3}), \\ f_c(t) &= \hat{f}\cos(\omega t + \theta_0 - \tfrac{4\pi}{3}), \end{aligned} \tag{3}$$

The term $\hat{f}$ refers to the amplitude of the signal, while θ_0 denotes to the phase angle, and ω represents the angular frequency.

Equations in (1) can be rewritten in the form of a single state phase, where it is represented by the imaginary unit corresponding to $i^2 = -1$

$$\vec{f} = \frac{2}{3}\left[e^{i0} f_{a\,(t)} + e^{i\frac{2\pi}{3}} f_{b\,(t)} + e^{i\frac{4\pi}{3}} f_{c\,(t)}\right] \tag{4}$$

$\vec{f}$ can be divided into real and imaginary components:

$$\vec{f} = f_{\alpha\,(t)} + i\, f_{\beta\,(t)} \tag{5}$$

where α represents the real components and β represents the imaginary components. By combining the real and complex components of (2) and (3), we obtain:

$$\begin{bmatrix} f_{\alpha\,(t)} \\ f_{\beta\,(t)} \end{bmatrix} = \begin{bmatrix} 1 & -\frac{1}{2} & -\frac{1}{2} \\ 0 & \frac{\sqrt{3}}{2} & -\frac{\sqrt{3}}{2} \end{bmatrix} \begin{bmatrix} f_a(t) \\ f_b(t) \\ f_c(t) \end{bmatrix} \tag{6}$$

The values of α and β change dynamically due to the rotating nature of the grid space frequency $\vec{f}(t)$. The vector α primarily varies along the real axis; the vector β varies along the imaginary axis. Therefore, the equation can be rewritten as follows:

$$\begin{aligned} f_\alpha(t) &= \hat{f}(t)\ \cos(\theta(t)) \\ f_\beta(t) &= \hat{f}(t)\ \sin(\theta(t)) \end{aligned} \tag{7}$$

The transformation from a three-phase domain to an alpha-beta domain reduces the system from three components to two components. However, the signals are still in a sinusoidal waveform.

The d-q domain provides a method to convert the oscillating control signal into DC waveforms by rotating the $\alpha - \beta$ with the frequency reference of AC signals during steady-state conditions. Which can be expressed mathematically by:

$$\begin{bmatrix} f_d(t) \\ f_q(t) \end{bmatrix} = \begin{bmatrix} \cos(\varphi) & \sin(\varphi) \\ -\sin((\varphi) & \cos(\varphi) \end{bmatrix} \begin{bmatrix} f_\alpha(t) \\ f_\beta(t) \end{bmatrix} \tag{8}$$

The combination of the two transformations provides a direct conversion from the three-phase domain into the dq-domain.

$$\begin{bmatrix} f_d(t) \\ f_q(t) \end{bmatrix} = \frac{2}{3} \begin{bmatrix} \cos(\varphi(t)) & \cos\left(\varphi(t) - \frac{2\pi}{3}\right) & \cos\left(\varphi(t) - \frac{4\pi}{3}\right) \\ \sin(\varphi(t)) & \sin\left(\varphi(t) - \frac{2\pi}{3}\right) & \sin\left(\varphi(t) - \frac{4\pi}{3}\right) \end{bmatrix} \begin{bmatrix} f_\alpha(t) \\ f_b(t) \\ f_c(t) \end{bmatrix} \tag{9}$$

Most of the PI controllers are utilized with the d-q domain since they provide better performance in controlling dc variables. The d-q control, also known as synchronous reference frame control, converts the grid currents from the abc frame to a d-q reference frame that rotates synchronously with the grid voltage (Parvez et al., 2016). Therefore, the sinusoidal signals are transformed into constant signals in the d-q reference frame. As illustrated in Figure 22, the transformation process from the three-phase AC signals (abc reference frame) to a two-axis reference frame dq-domain.

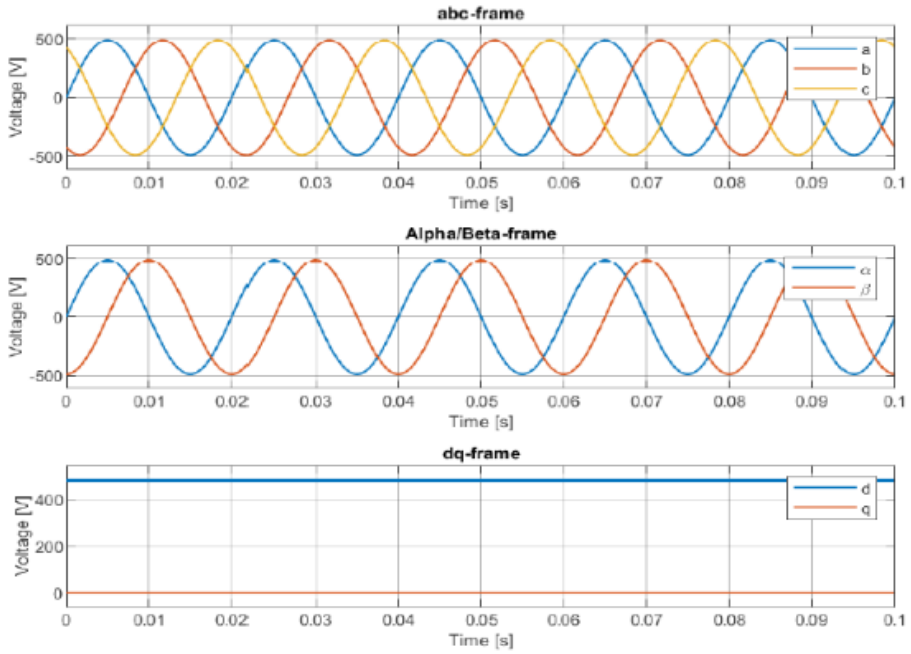

Figure 22. Transformation from a three-phase domain to αβ and dq domains (Roos, 2020).

4.2 Simulink model of grid-tied inverter

The initial step for implementing the grid compliance model in Chapter 5 involves modeling the inverter using MATLAB Simulink. The aim is to develop a grid emulator for grid codes compliance during overvoltage, undervoltage, over-frequency, and under-frequency scenarios. To assess the inverter's ability to withstand grid faults, a voltage signal

will be extracted from the output of the LCL filter, which is the point of measurement, to test the capability of the inverter to ride through faults.

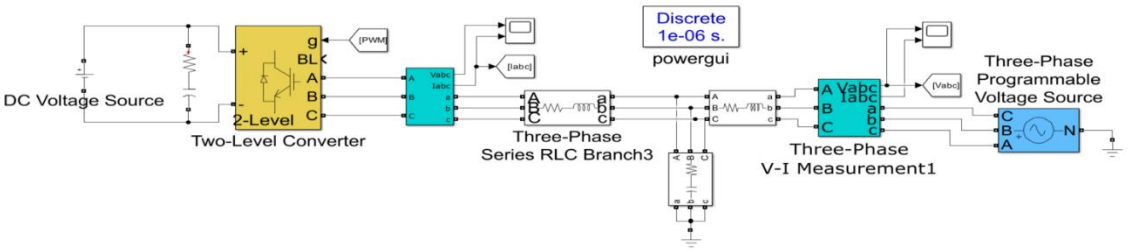

Figure 23. Simulink model of a grid-tied inverter.

The ideal DC voltage source is utilized with an amplitude of 800V, which represents the energy produced from RES connected to the two-level inverter. The inverter is modeled using a switching function controlled by a pulse width modulation (PWM) generator. The ideal three-phase voltage and current measurement block is used to verify the inverter signal before and after the filter. The block can measure phase-to-phase voltages or phase-to-ground voltages. In this case, phase-to-phase voltage measurement is used. Then, a three-phase RLC branch is used to implement the LCL filter to reduce the harmonics of the inverter. A three-phase programmable voltage source is used as an emulate.

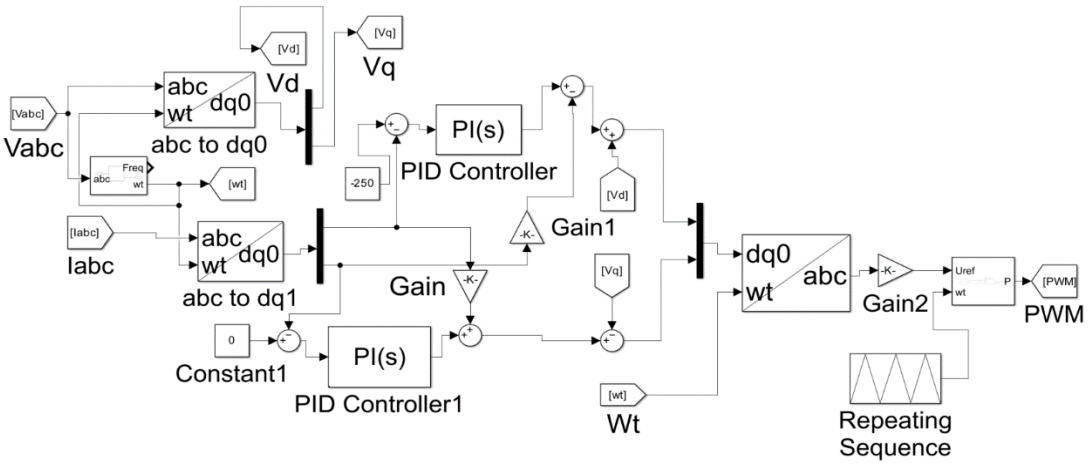

Figure 24. The current controller circuit - Simulink.

A PLL control system is implemented to synchronize the output waveforms of the inverter. The three-phase abc domain is transformed into a two-phase (α-β domain) using the Park transformation. $\alpha - \beta$ domain is converted to a dq domain using the Clarke transformation (Corporation, 2013).

Figure 25 illustrates the simulation results of the grid voltage and inverter current. The grid voltage is the voltage that is supplied by the electrical grid, and the inverter current refers to the electrical current produced by the inverter. The vertical axis of the graph represents the voltage and current measured in voltage and current, respectively, while the horizontal axis represents the time in seconds.

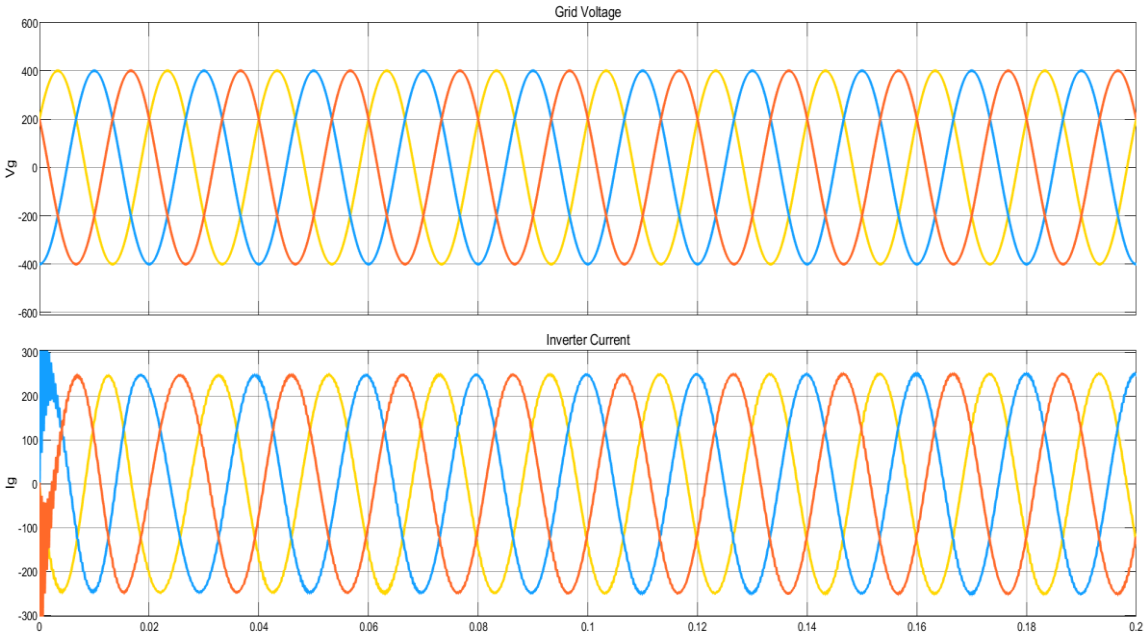

Figure 25. Grid voltage and inverter output current

5 Simulation model

This chapter introduces the main simulation model of this thesis. The aim is to provide a simulation-based grid code compliance testing model for the inverter model implemented in Chapter 4. The primary goal is to develop a grid emulator for grid codes compliance, to evaluate the compliance of the inverter during overvoltage and under-voltage simulations, as well as over-frequency and under-frequency scenarios

Integrating RES into the grid is a crucial step towards a sustainable future. However, ensuring their compliance with grid codes before integrating them is a significant challenge. Therefore, grid code compliance testing is a mandatory process. Simulation-based compliance tests offer a time-saving and cost-effective alternative. However, simulation-based testing offers many advantages. It enables the emulation of real-life scenarios without the need to connect to the actual grid. This enhances safety during implementing the tests by reducing the risk of causing damage to the equipment under the tests (EUT).

5.1 UVRT and OVRT tests

In this chapter, a simulation-based compliance testing process is implemented utilizing MATLAB Simulink to evaluate compliance with grid codes. Figure 26 illustrates the process of implementing UVRT and OVRT tests based on EN50549-1, EN50549-2, and EN50549-10 standards. The test provides a comprehensive comparison between the signal of the inverter, the OVRT and UVRT thresholds, and the trip signal to ensure that the trip signal operates exactly when the voltage violates the thresholds. Figure 26 illustrates the process of implementing the simulation model.

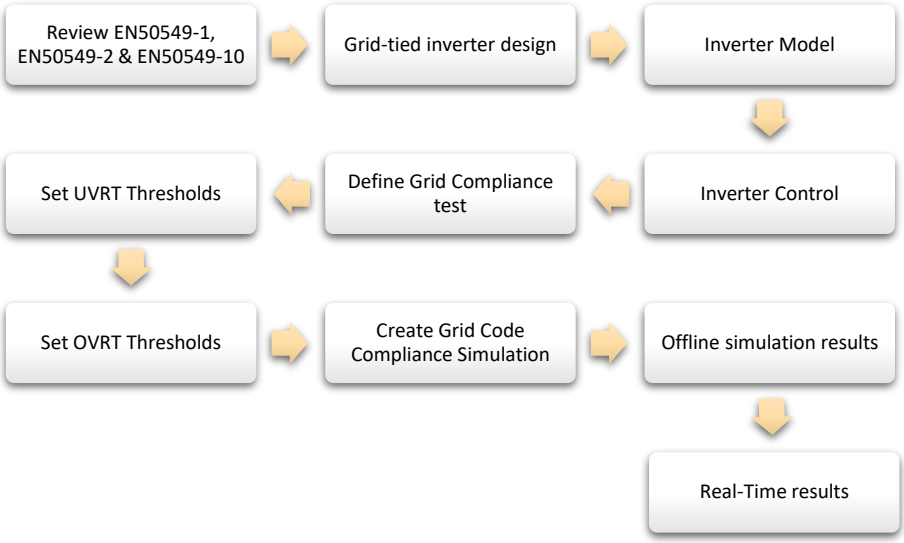

Figure 26. Testing process.

The DC source of the simulation model in Figure 27 represents renewable energy resources such as solar power or wind turbines connected to a three-phase inverter. The output of the inverter is connected to the LCL filter, which is connected to the three-phase voltage measurement. This is considered the point of measurement as per the standards EN50549-1 and EN50549-2 standards. A three-phase programmable voltage source is used as a grid emulator.

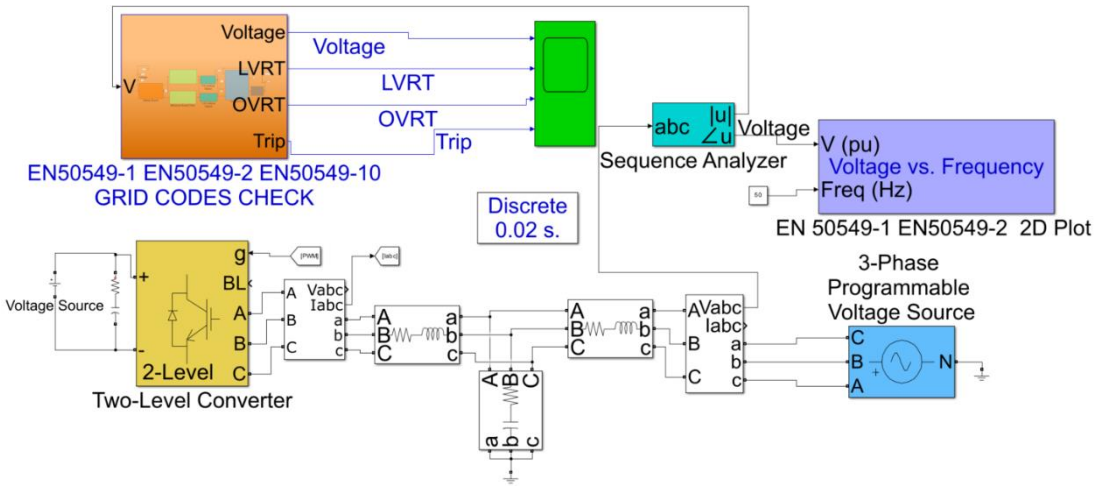

Figure 27. Simulation-based grid compliance tests.

The signal taken from the V-I voltage measurement is a three-phase signal. However, the magnitude of the signal in p.u. is required to perform UVRT and OVRT tests. Thus, the sequence analyzer block is used to convert the output of the three-phase signal to the magnitude and phase of the signal. The signal is taken from the sequence analyzer to the grid code check block.

A three-phase programmable zero-impedance voltage source is employed as a grid emulator that can create UVRT and OVRT events. It enables the adjustment of the amplitude of the voltage signal over various time periods. This allows for creating a fault event for a specific duration and subsequently restores the voltage to its normal operating condition. To perform UVRT and OVRT events for the specific time required for each test.

The aim is to conduct compliance testing based on the thresholds specified in EN50549-1 and EN50549-2 standards. The LeSage (2024) grid code simulation model has been modified to be compatible with the standards. The output signal of the inverter is compared with the specified UVRT and OVRT thresholds. To verify that the system operates under the required conditions. A Simulink scope with four outputs has been used to facilitate the comparison process between voltage signals, UVRT and OVRT thresholds, and the trip signal. To directly compare the voltage signal with UVRT and OVRT thresholds, and to ensure that the trip signal is activated precisely at the required time, without early or delayed trips, remains at either 0 or 1. The trip signal remains at 0 as long as the inverter voltage stays within the UVRT and OVRT thresholds. However, once the inverter signal violates the predefined thresholds, the trip signal activates and shifts to 1, and remains at that state to prevent continuous system triggering.

The grid code check system in Figure 28 consists of a series of interconnected subsystems used to test the compatibility of the inverter. Each system has a task to conduct the tests. The "Detect Event" subsystem is the first step within the grid code check block. This subsystem utilized pre-determined thresholds to detect under-voltage and over-voltage events by using relational operators, as illustrated in Figure 29. A voltage dip is detected

when the voltage falls below 0.9 p.u., and a voltage rise event is detected when the voltage exceeds 1.1 p.u.

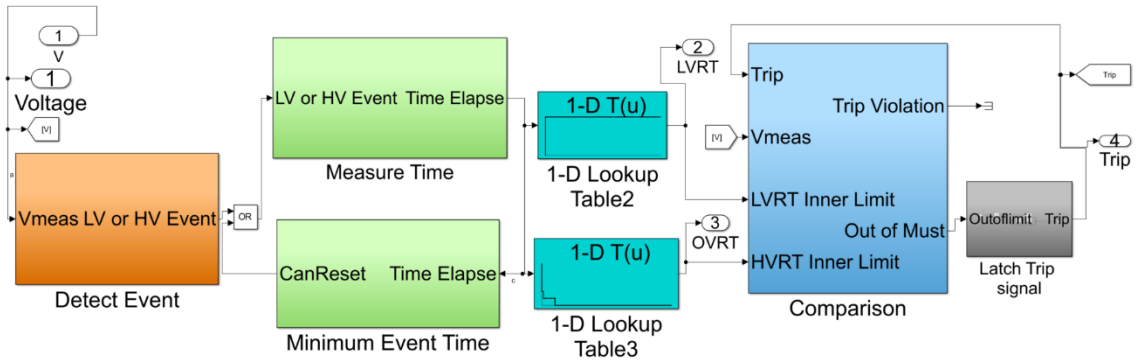

Figure 28. Grid code check system block.

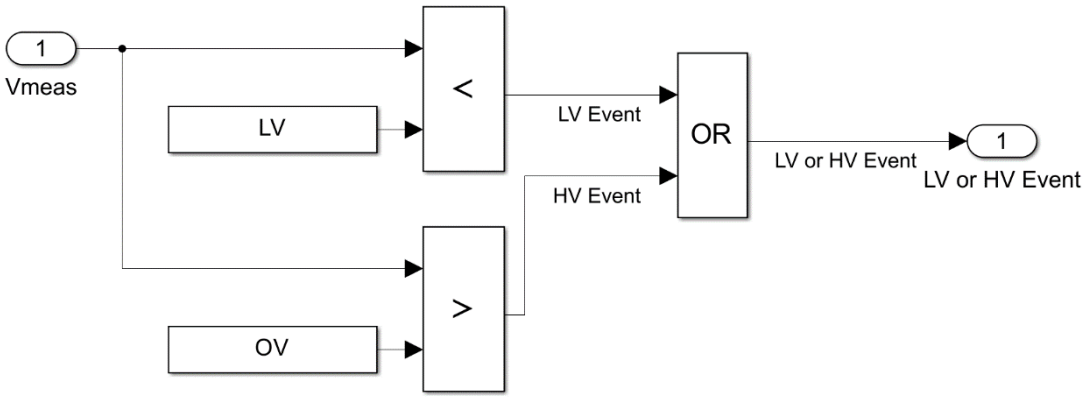

Figure 29. Detect event subsystem.

The output signal from the "Detect Event" is connected to two subsequent subsystems, "Measure Time and Minimum Time Event". As illustrated in Figure 28. This subsystem consists of a timer and an integrator, as shown in Figure 30. Upon the detection of an under voltage or over voltage event, the system triggers to initiate the timer. The "Minimum Event Time" subsystem shown in Figure 31 is used to function as the reset of the timer.

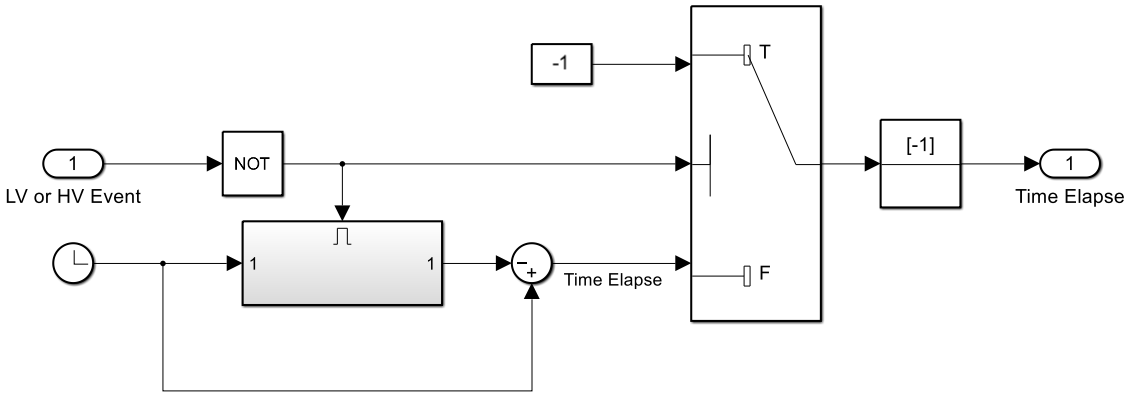

Figure 30. Measure time subsystem.

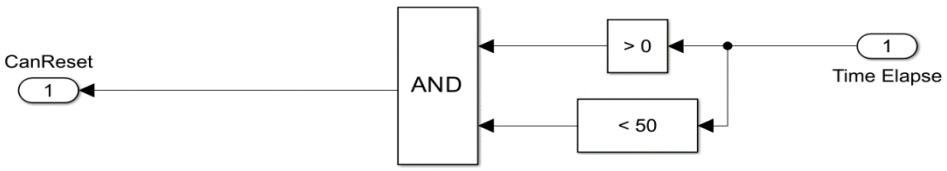

Figure 31. Minimum time event.

Following the timer and the reset subsystems, the output will then enter the lookup tables, which are used to set the voltage and time thresholds of UVRT and OVRT events. These thresholds will then be compared with the inverter signal. Threshold can be defined directly within the lookup tables within the Simulink model or through a separate MATLAB script.

Comparison is the final subsystem that compares the voltage in an event with the defined voltage and time thresholds to decide the activation time of the trip signal. Relational operators are employed to compare the event with the UVRT and OVRT thresholds.

In the comparison subsystem, the voltage in an event will be compared with UVRT and OVRT thresholds using relational operators, as depicted in Figure 32. The "AND" logical

operator is used to define the area between the thresholds, which is the normal operating region, which is the area between OVRT and OVRT. As long as the voltage signal falls within this threshold, which is defined as "BetweenLVHV", the trip signal will remain inactive. However, if the signal of the inverter falls outside the "BetweeLVHV" region, the trip signal should activate. Moreover, if the trip signal is activated, it should remain in that state to prevent continuous system triggers.

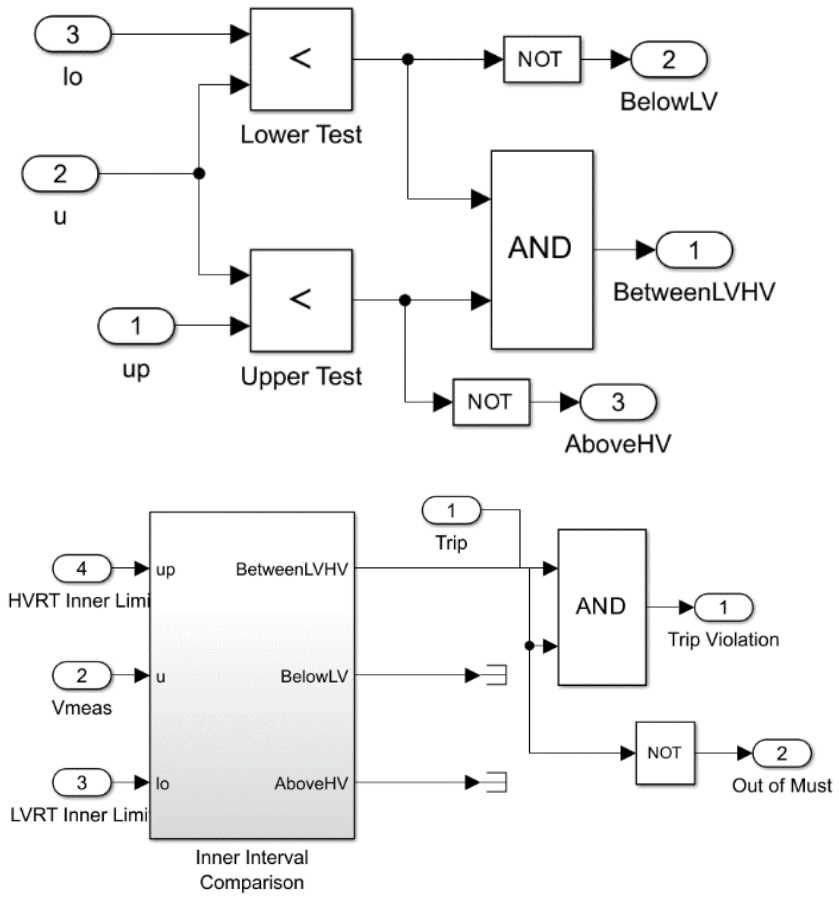

Figure 32. Comparison subsystem.

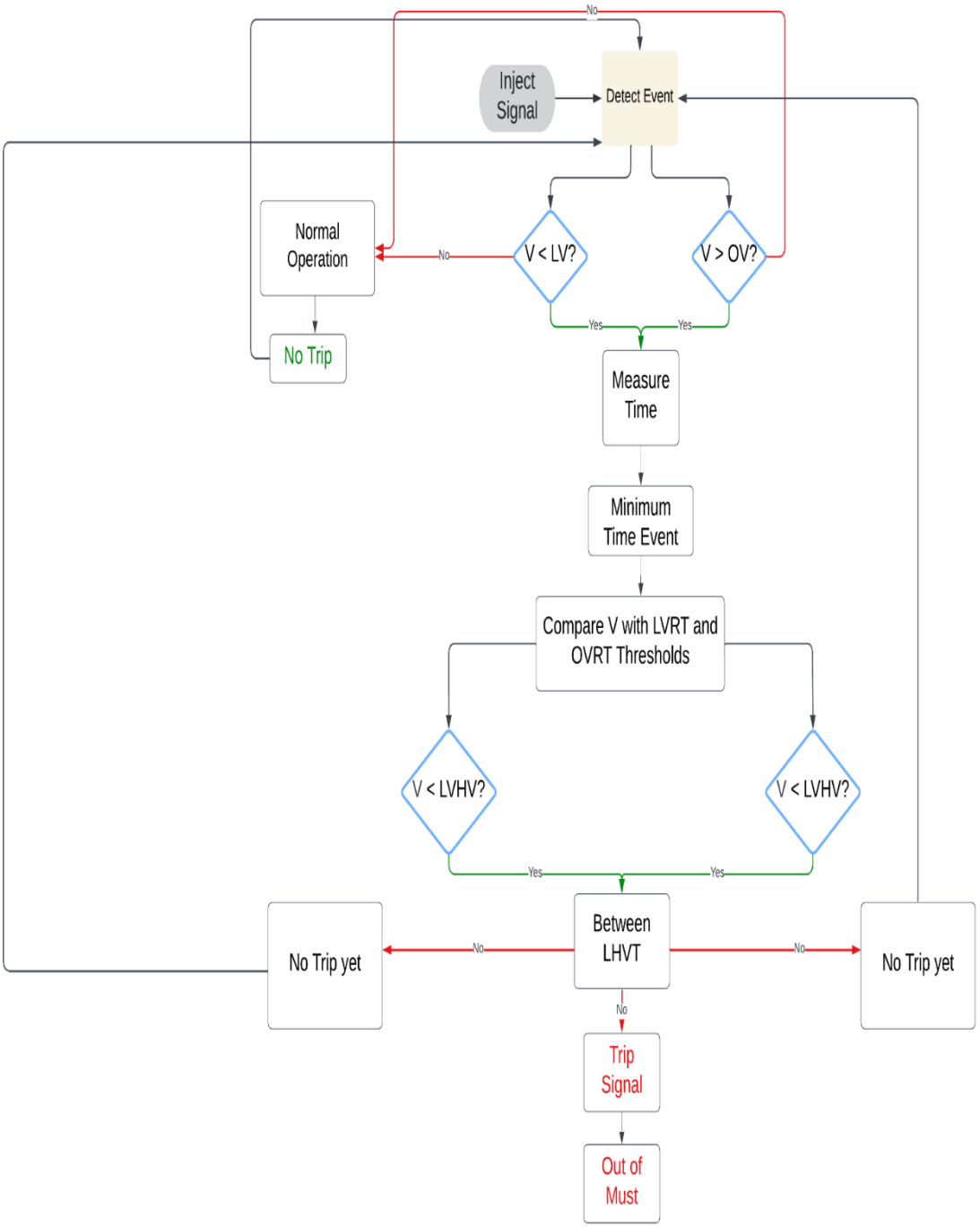

Figure 33. Flowchart of the process.

The voltage vs. frequency block in Figure 34 contains a MATLAB function that plots the voltage and the frequency over different time intervals. The purpose of this function is to monitor the voltage and frequency of the system throughout the entire simulation period. It enables the ability to monitor the performance of the system by showing how

the frequency and voltage vary from the nominal values to prevent unfavorable events to the grid, which helps to understand the system's dynamics and improve its reliability. Figure 34 illustrates the flowchart that provides an explanation of the MATLAB code in Appendix 1.

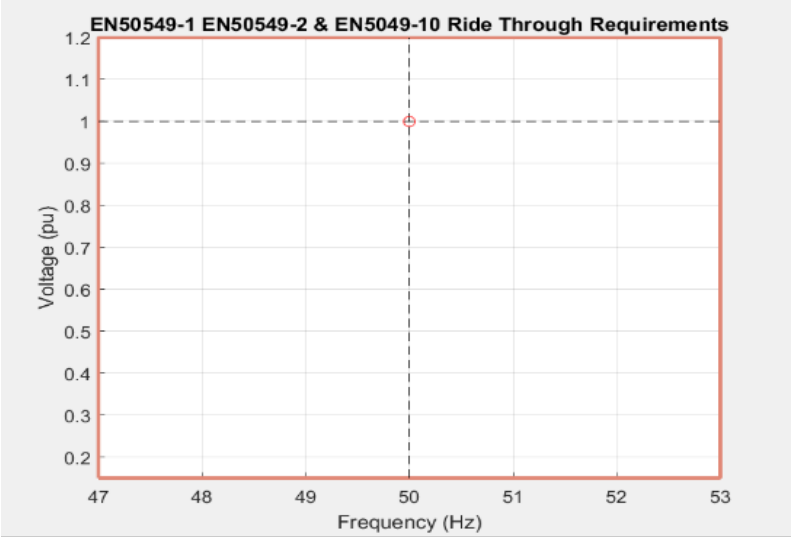

Figure 34. Voltage versus frequency graph.

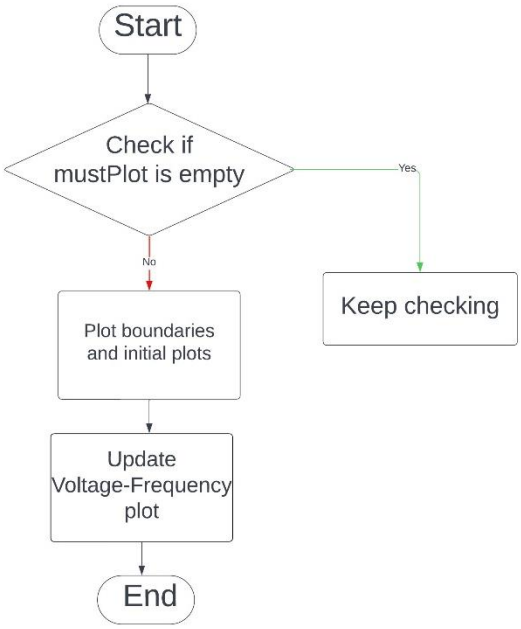

Figure 35. Flow chart of the MATLAB function.

5.2 Over frequency and under frequency tests

Frequency compliance testing is performed in MATLAB Simulink using a frequency relay block developed by Tan (2021). The system consists of a programmable voltage source, a frequency relay, and a three-phase circuit breaker. The simulation model enables the simulation of frequency variations over time.

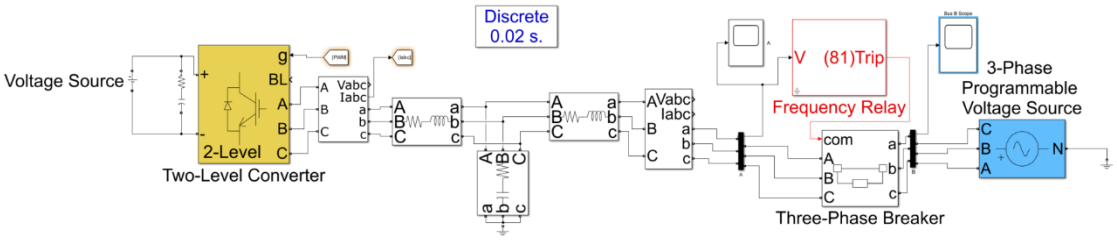

Figure 36. Frequency compliance testing (Rodney Tan, 2021).

Based on the EN50549-1 standard, the generating plant should have the capability to operate when the frequency range at the POC is between 49 Hz and 51 Hz. In addition, the generating modules should have the capability to remain connected if the frequency in the operating zone occurs between 47 Hz and 52 Hz until the safety breaker is activated.

The initial phase of the test is to define the frequency of the simulation model at 50 Hz. The next step is to define the normal operating frequency of the system in the programmable voltage source and the frequency relay. Subsequently, initiating an over-frequency and under-frequency event using the programmable voltage source that is capable of emulating the frequency of the system, allows determining the values required to conduct the test.

Under and over frequency settings can be adjusted within a range of 1% to 20% in the frequency relay block. Table 4 demonstrates the configuration and the corresponding changes in frequency utilizing the frequency relay block. The frequency relay will activate

whenever the frequency deviation reaches the thresholds. For example, if the under-frequency setting is defined at 5%, the frequency relay will operate once the frequency in the system reaches 47.5 Hz or 52.5 Hz. Then a signal will be transmitted from the frequency relay to activate the three-phase circuit breaker.

Table 4. Configurations of the frequency relay.

Adjustment	variation
$\pm 1\%$	0.5Hz
$\pm 2\%$	1.0Hz
$\pm 3\%$	1.5Hz
$\pm 4\%$	2Hz
$\pm 5\%$	2.5Hz

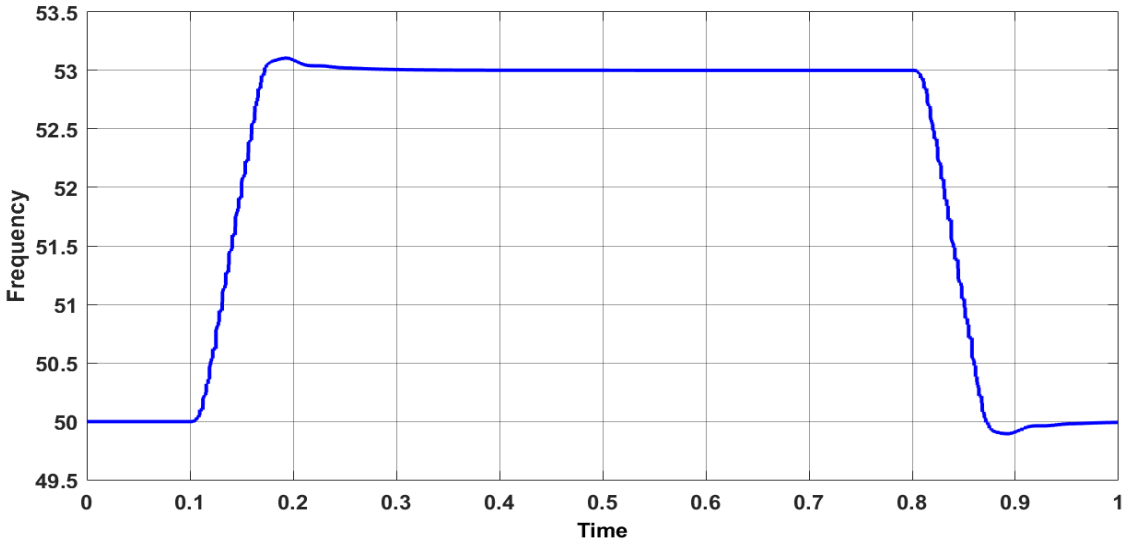

Figure 37. Frequency variation graph.

6 Results and discussions

This chapter includes the results obtained from the simulation models in Chapter 5 that are used to test the compatibility of the inverter with grid codes. This chapter also includes a brief introduction to the real-time simulation and the real-time simulation results obtained using the OPAL-RT real-time simulator.

The purpose of the test is to demonstrate the ability of the inverter to withstand non-significant voltage fluctuations over specific durations. As shown in the voltage-time curve, there are three zones that require testing. To prove compliance, at least two tests must be conducted for each area, according to standard EN50549-10.

6.1 UVRT results

Figure 38 illustrates the UVRT threshold that the generating models should be capable of maintaining connection with the gid. To demonstrate the compatibility of the simulation results, the thresholds are divided into three zones, and a minimum of two tests will be conducted in the next section to evaluate the results of the simulation model.

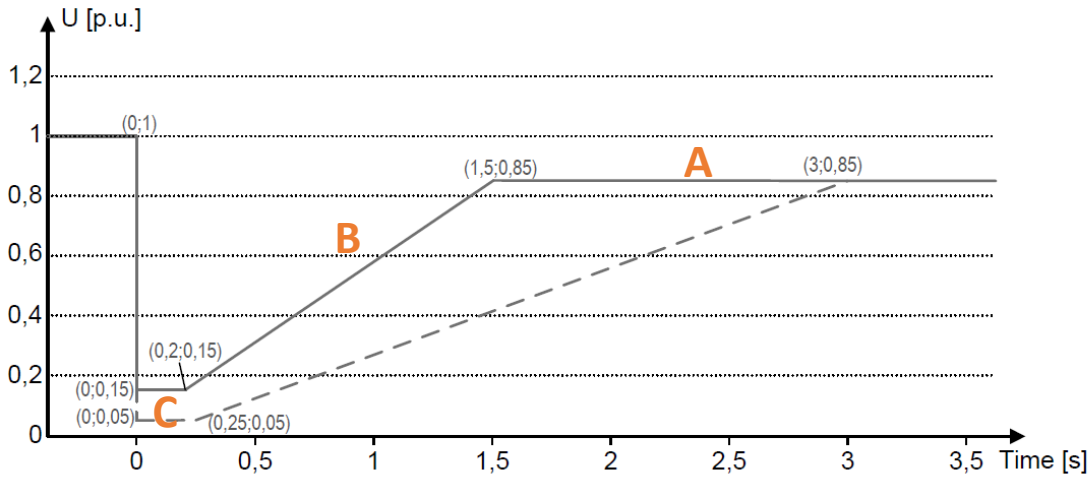

Figure 38. UVRT test thresholds.

6.1.1 Zone A

The x-axis in Figure 39 represents the time in seconds, while the y-axis is the voltage per unit (p.u.). The graph illustrates the voltage signal (green line), UVRT thresholds (red line), and trip signal (purple line). When the voltage signal violates the UVRT threshold, the trip signal will switch from zero to 1, which indicates that the inverter should be disconnected from the grid. Otherwise, the trip signal will remain at zero, which indicates the ability of the inverter to remain connected to the grid. In zone A, the voltage should not remain below 0.85 p.u. for 1.5 seconds or more.

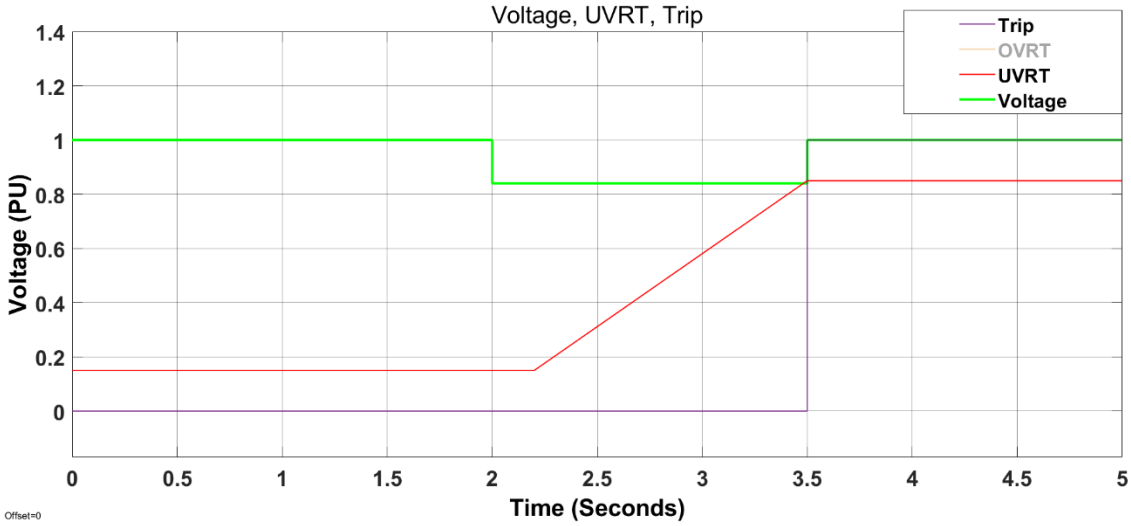

Figure 39. 0.84 p.u. for 1.5 seconds.

In the UVRT scenario depicted in Figure 39, the voltage started at the nominal operating level (1 p.u.) for 2 seconds. Then it decreased to 0.84 p.u. from the nominal value and remained for a duration of 1.6 seconds. This duration is below the voltage threshold for zone A. Therefore, it indicates that the inverter should be disconnected from the grid. Consequently, the trip signal is activated exactly when the signal violates the UVRT threshold.

In the UVRT scenario depicted in Figure 40, the voltage started at the nominal operating level of 1 p.u. for 2 seconds. Then a fault occurs and causes a decrease to 0.84 p.u. from the nominal value, sustained for a duration less than 1.5 seconds. In this scenario, the voltage remains above the UVRT voltage and time threshold specified for zone A. Therefore, as defined by the standard, the inverter should have the ability to remain connected to the grid. Thus, the trip signal remains at zero, indicating that it is not active.

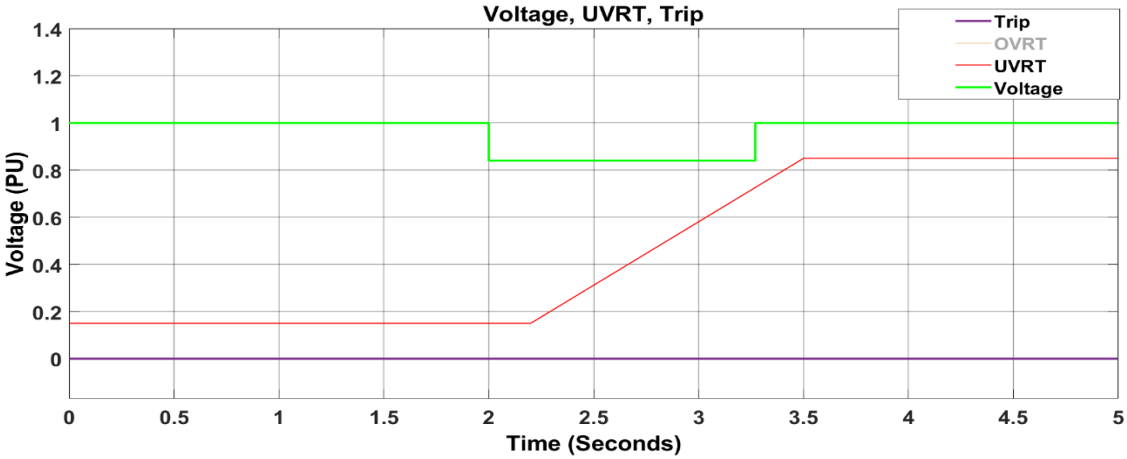

Figure 40. 0.84 p.u. for less than 1.5 seconds.

6.1.2 Zone B

The maximum acceptable voltage drop thresholds are as follows: 0.4 p.u. for less than 0.4 seconds, 0.6 p.u. for less than 0.8 seconds and 0.8 p.u. for less than 1.3 seconds.

In the UVRT test scenario depicted in Figure 41, the voltage started at the nominal operating level for 2 seconds. Then a fault occurs, causing a voltage decrease from the nominal value to 0.6 p.u., and sustained for a duration of less than 1 second. The voltage signal falls close to the UVRT threshold but does not violate it. Therefore, the inverter should be capable of remaining connected; as illustrated in the graph, the trip signal did not operate.

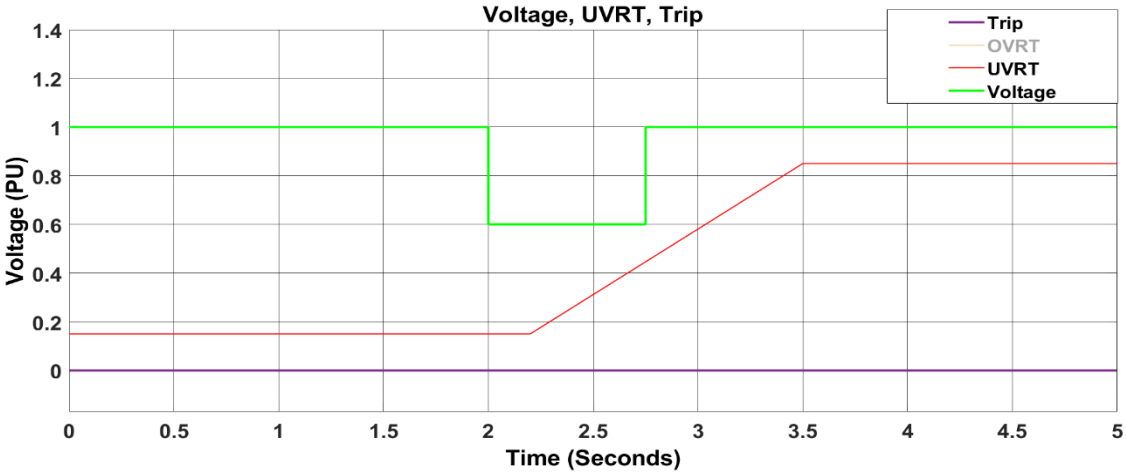

Figure 41. 0.6 p.u. for less than one second.

In the UVRT test scenario depicted in Figure 42, the voltage started at the nominal operating level (1 p.u.) for 2 seconds. Then, a fault occurs and causes a decrease in voltage from the nominal value to 0.6 p.u., for more than one second. As illustrated in the graph, the voltage dropped below the UVRT region. In this case, the generating modules must be disconnected. Therefore, the trip signal was activated precisely at the moment when the voltage signal violated the UVRT threshold.

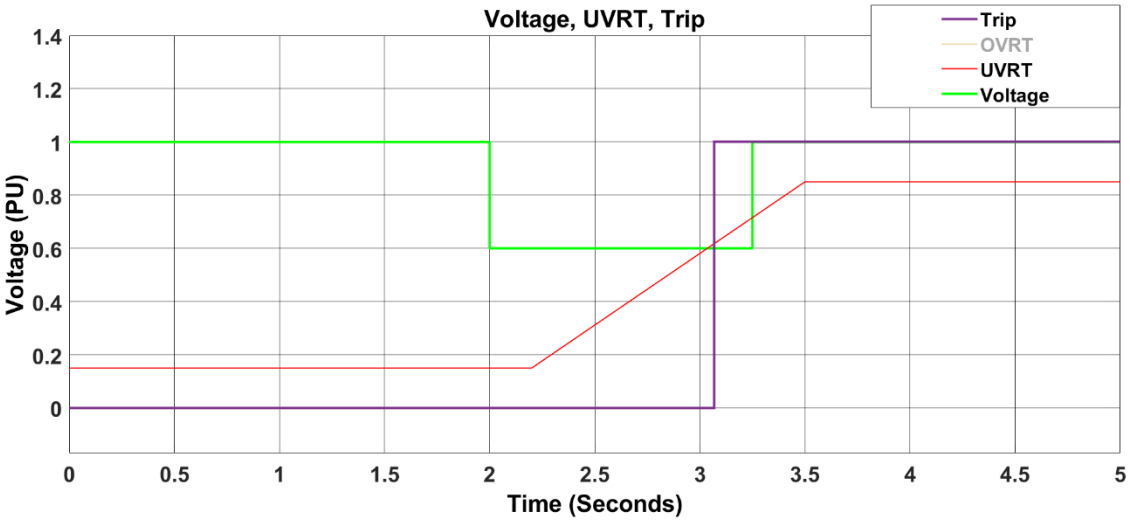

Figure 42. 0.6 p.u. for 1.25 seconds.

In the UVRT test scenario illustrated in Figure 43, the voltage begins at the nominal operating level for 2 seconds. A fault occurs and causes a decrease in the voltage from the nominal value to 0.4 p.u. for a duration of 0.2 seconds. The voltage in this case did not cross the UVRT region. In this scenario, the generating modules should be capable of remaining connected, and as expected, the trip signal did not operate.

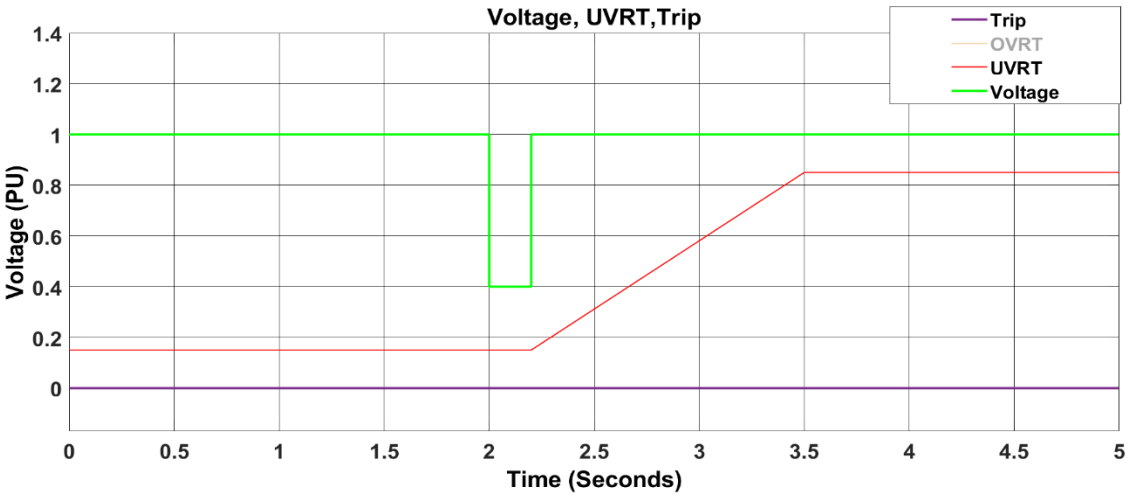

Figure 43. 0.4 p.u. for 0.2 seconds.

6.1.3 Zone C

In the UVRT test scenario illustrated in Figure 44, the voltage started at the nominal operating level for 2 seconds. Then, a fault occurs and causes a decrease in the voltage from the nominal value to 0.15 p.u., which is sustained for a duration of 0.2 seconds. As illustrated in the graph, the voltage dips below the UVRT region. In this case, the generating modules should be disconnected. Therefore, the trip signal was activated exactly at the moment when the voltage signal violated the UVRT threshold.

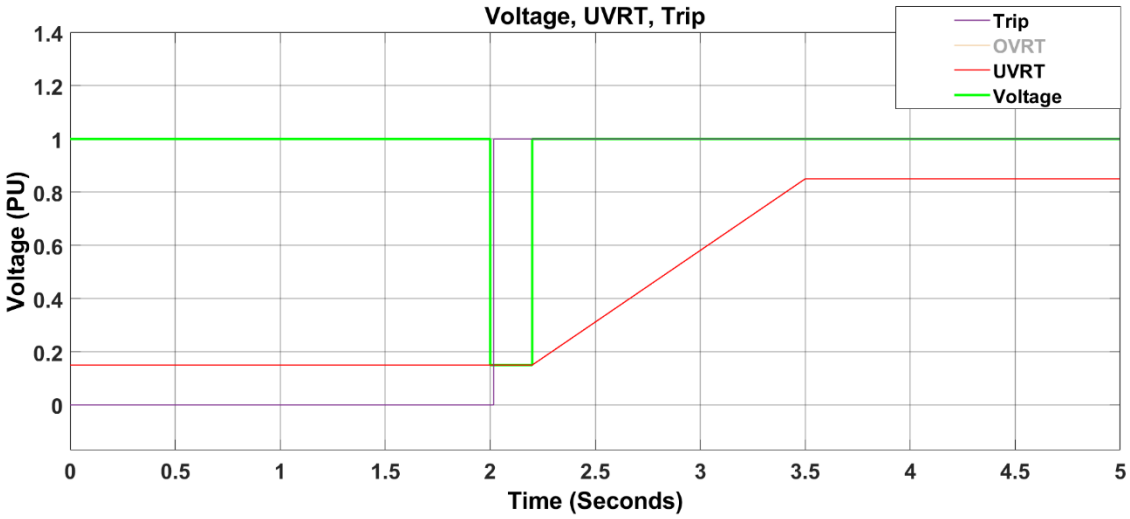

Figure 44. 0.15 p.u. for 0.2 seconds.

In the UVRT test scenario illustrated in Figure 45, the voltage begins at the nominal operating level for 2 seconds. A fault then disrupts the system, causing a voltage dip to 0.17 p.u. for a duration of 0.15 seconds. As the voltage remains above the UVRT thresholds, the inverter should be connected to the grid, and accordingly, the trip signal remains inactive.

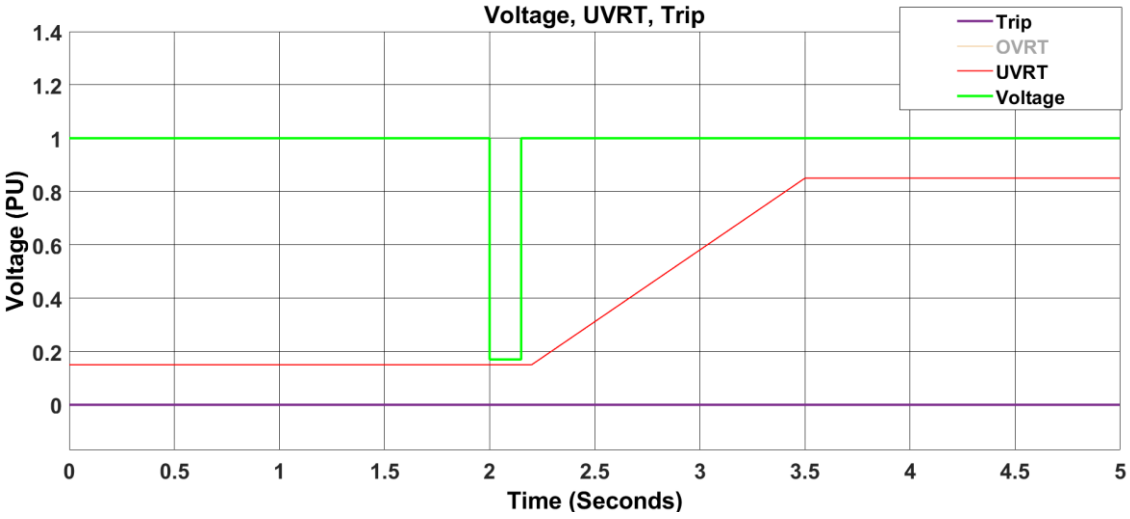

Figure 45. 0.17 p.u. for 0.15 seconds.

6.2 OVRT results

Similar to the UVRT thresholds, the OVRT thresholds are depicted in Figure 46, which outlines that the generating models should be capable of remaining connected to the grid. To validate the simulation results' compatibility, these thresholds are divided into three zones. Furthermore, a minimum of two tests will be carried out in the following section to evaluate the simulation model results.

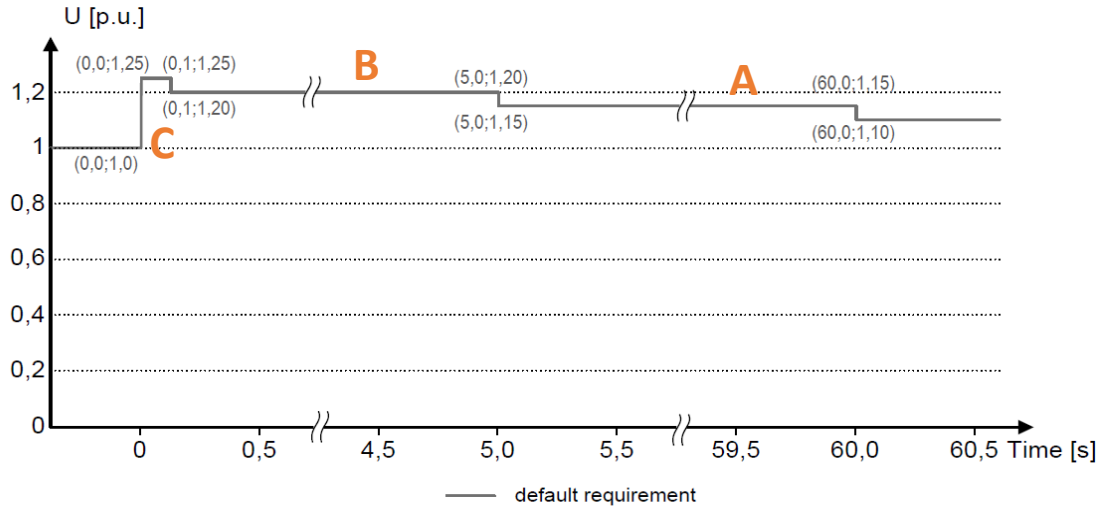

Figure 46. OVRT test zones.

6.2.1 Zone A

Testing the OVRT capability as per zone A: the voltage can increase to a value less than 1.15 p.u. and remain for less than 55 seconds. In the OVRT test scenario depicted in Figure 47, the voltage started at the nominal operating level for 10 seconds. Then the voltage increased from the nominal value to 1.13 p.u. and sustained for a duration of 50 seconds, which indicates an over-voltage condition. However, it did not violate the OVRT thresholds. Therefore, the trip signal did not operate, and the inverter could remain connected to the grid.

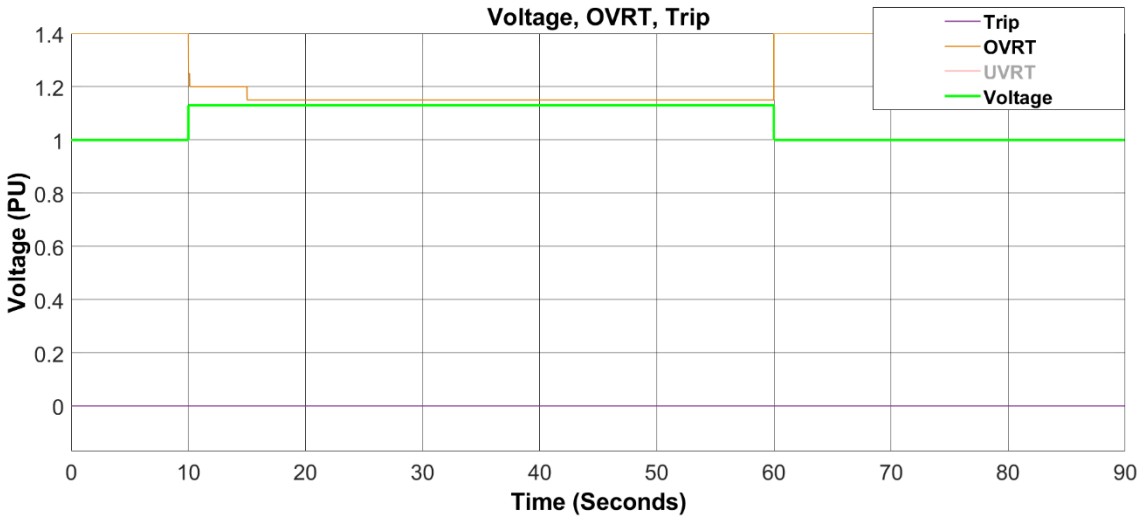

Figure 47. 1.13 p.u. for 50 seconds.

In the OVRT test scenario illustrated in Figure 48, the voltage started at the nominal operating level for 10 seconds. Then the voltage increased from the nominal value to 1.17 p.u. and was sustained for a duration of 50 seconds. As illustrated in the graph, the voltage crossed the OVRT threshold. Therefore, the generating modules should be disconnected, and as expected, the trip function was activated exactly at the moment when the voltage signal violated the UVRT threshold.

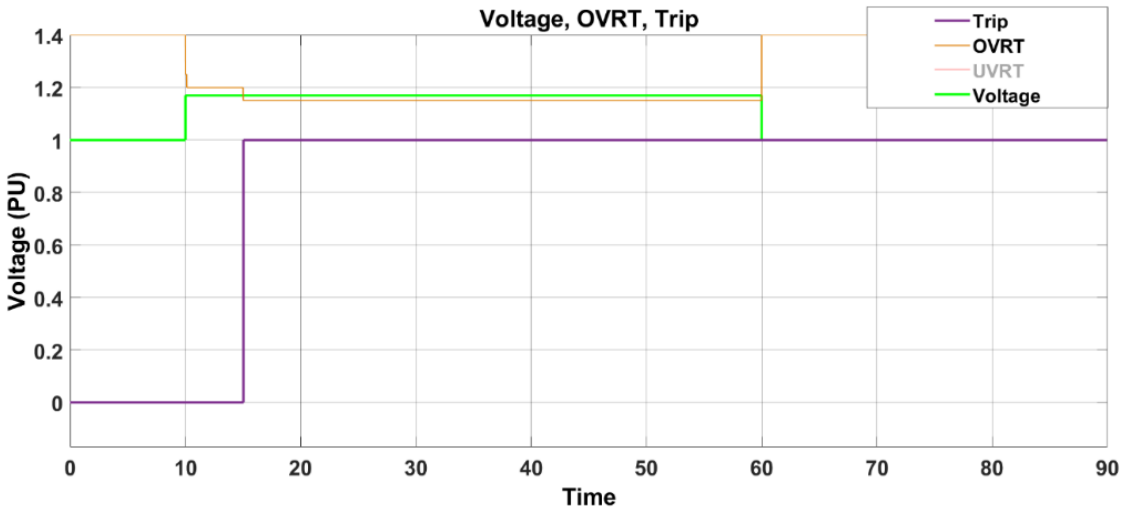

Figure 48. 1.17 p.u. for 50 seconds.

6.2.2 Zone B

In this zone, the voltage is allowed to increase to a value less than 1.20 p.u. for a duration of less than 5 seconds. If the voltage increases to 1.20 p.u. or remains for more than 5 seconds, the trip function should operate.

In the OVRT test scenario depicted in Figure 49, the voltage started at the nominal operating level for 0.5 seconds. Then the voltage increased from the nominal value to 1.14 p.u. and was sustained for a duration of 4 seconds, which is within the acceptable threshold. Therefore, the grid should still be connected, and as expected, the trip signal did not operate.

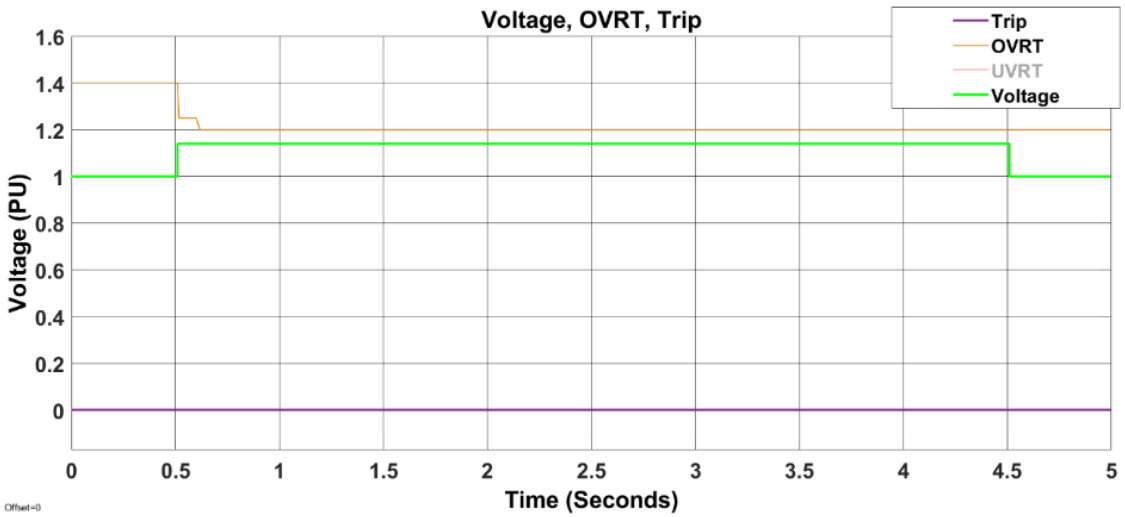

Figure 49. 1.14 p.u. for 4 seconds.

In the OVRT test scenario depicted in Figure 50, the voltage started at the nominal operating level for 0.5 seconds. Then it increased from the nominal value to 1.21 p.u. for a duration of 4 seconds. As indicated in the graph, the voltage crossed the OVRT region. Therefore, the generating modules should be disconnected according to grid code requirements. Consequently, the trip function was activated when the voltage signal violated the UVRT threshold.

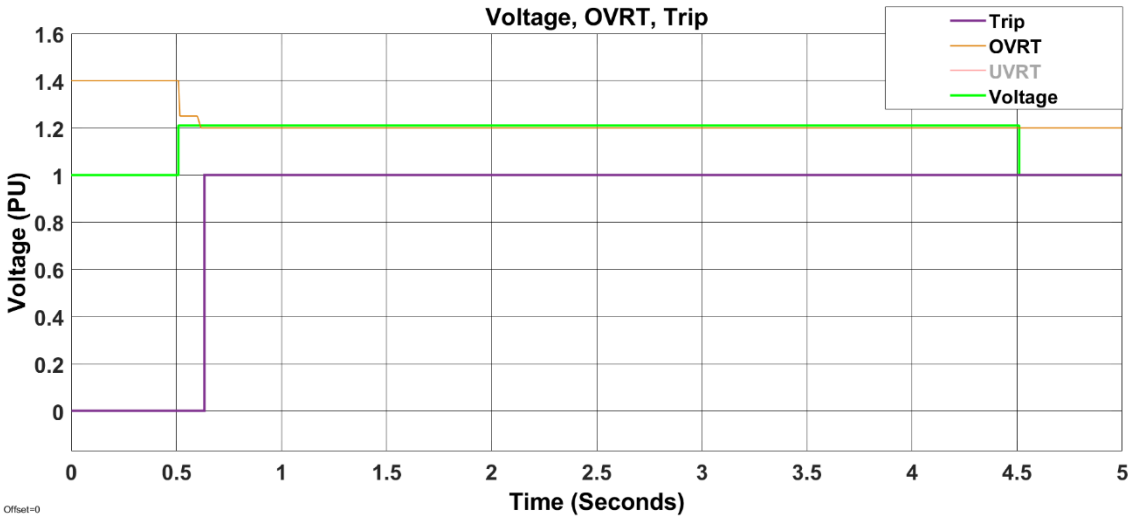

Figure 50. 1.21 p.u. for 4 seconds.

6.2.3 Zone C

In the OVRT test scenario illustrated in Figure 51, the voltage began at the nominal operating level for 0.4 seconds. Then the voltage increased from the nominal value to 1.23 p.u. and was sustained for a duration of less than 0.1 second. While the voltage approached the OVRT closely, it did not violate it. As indicated in the graph, it would have tripped if the voltage increased to 1.25 p.u.

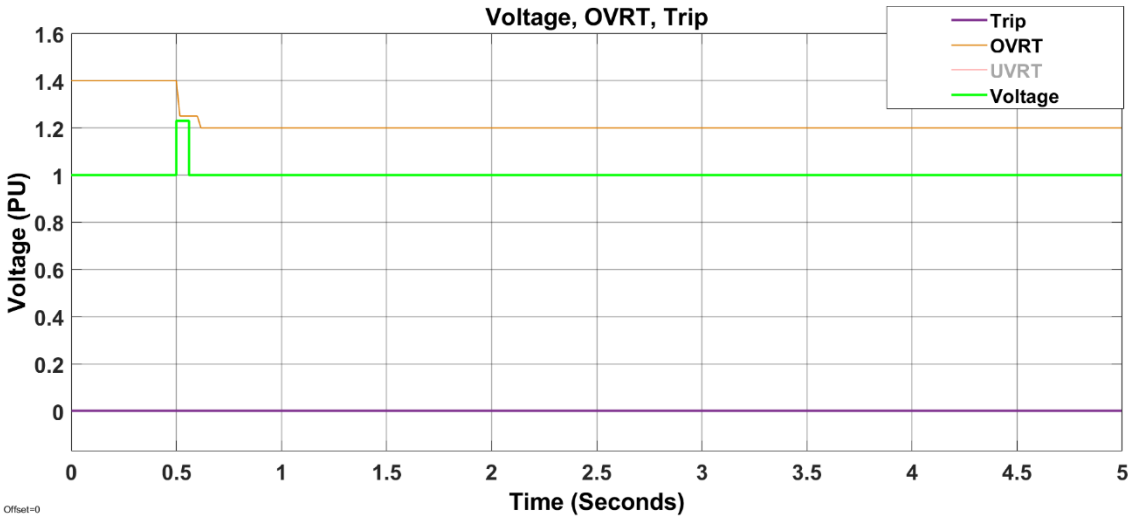

Figure 51. 1.23 p.u. for less than 0.1 second.

In the OVRT test scenario depicted in Figure 52 above, the voltage began at the nominal operating level for 0.4 seconds. The voltage then increased from the nominal value to 1.24 p.u. and sustained for more than 0.1 second. While the voltage is still below 1.25 p.u. threshold, it violated the second condition of zone C by remaining for more than 0.2 seconds. Therefore, the trip signal was activated.

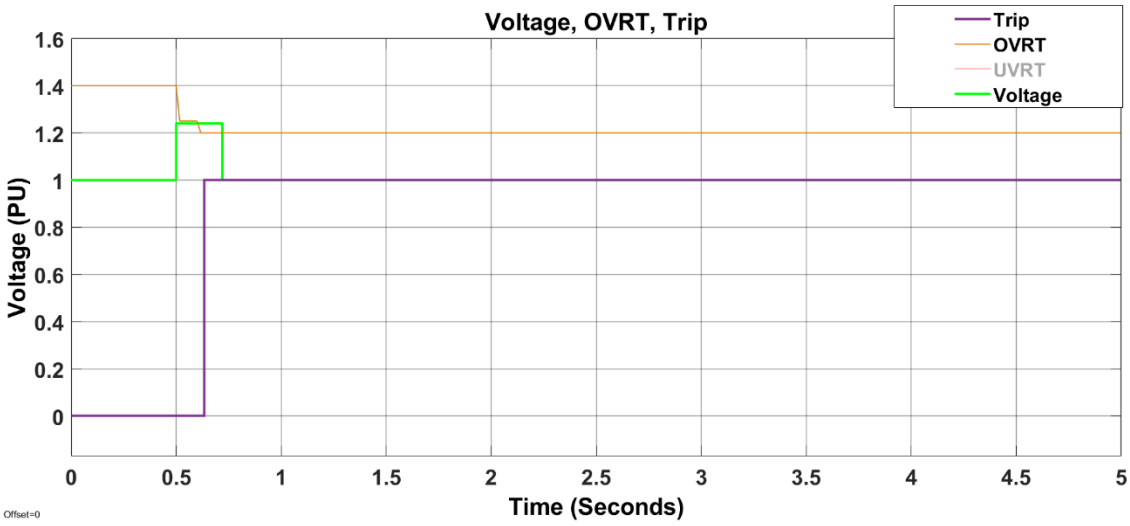

Figure 52. 1.23 p.u. for less than 0.1 second.

The x-axis in Figure 53 represents the time in seconds, while the y-axis is the voltage per unit (p.u.). The graph illustrates the voltage signal (green line), UVRT thresholds (red line), and trip signal (purple line). When the voltage signal violates the UVRT threshold, the trip signal will switch from zero to 1, which indicates that the inverter should be disconnected from the grid. Otherwise, the trip signal will remain at zero, which indicates the ability of the inverter to remain connected to the grid. In the OVRT test scenario depicted in Figure 53, the voltage started at the nominal operating level for 0.4 seconds. Then the voltage increased from the nominal value to 1.24 p.u. and sustained for more than 0.1 second, which is less than the 1.25 p.u. threshold in zone C. However, the second condition is to remain for less than 0.2 seconds. As illustrated in the graph, the signal of the inverter violated the OVRT threshold. Therefore, the trip signal was activated.

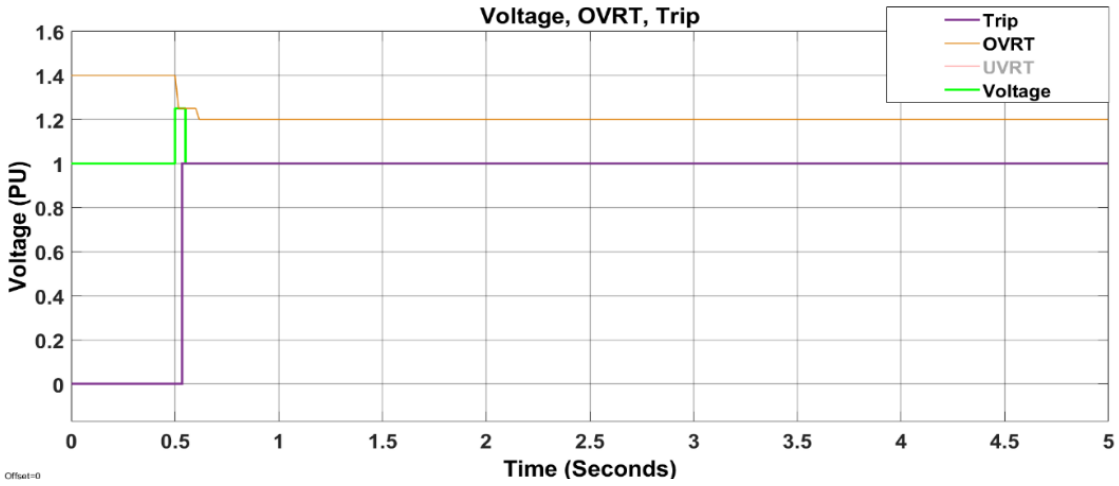

Figure 53. 1.25 p.u. for more than 0.1 second.

6.3 Frequency test results

6.3.1 Under frequency test results

As illustrated in Figure 54, frequency variation event of 47 Hz was achieved by emulating the frequency of the system to a value of 47 Hz. The frequency relay was configured to operate when the under-frequency condition reaches 47.5 Hz. Upon reaching this threshold, the frequency relay will send a signal to activate the three-phase circuit breaker and disconnect the grid. In this case, the delay was set to 0.40 seconds. Therefore, the grid was disconnected in 0.4 seconds, as illustrated in Figure 55 (Tan, 2021).

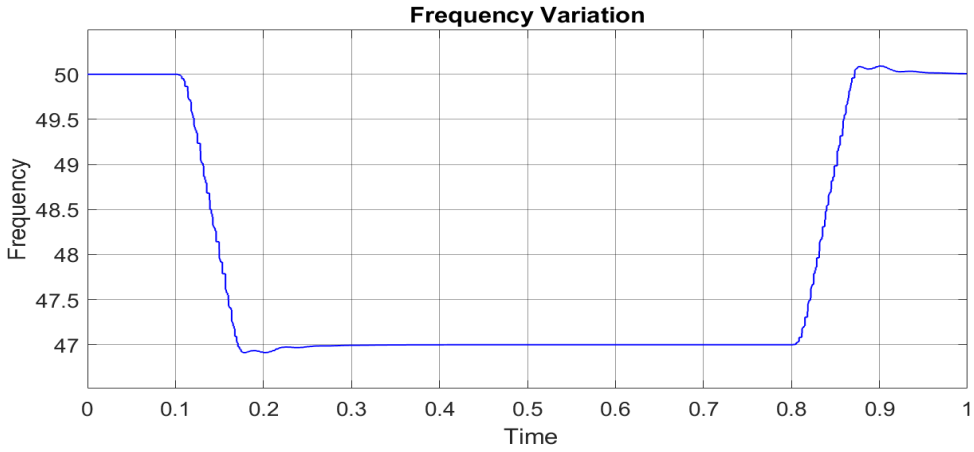

Figure 54. frequency reaches 47 Hz which activates the frequency relay (Tan, 2021).

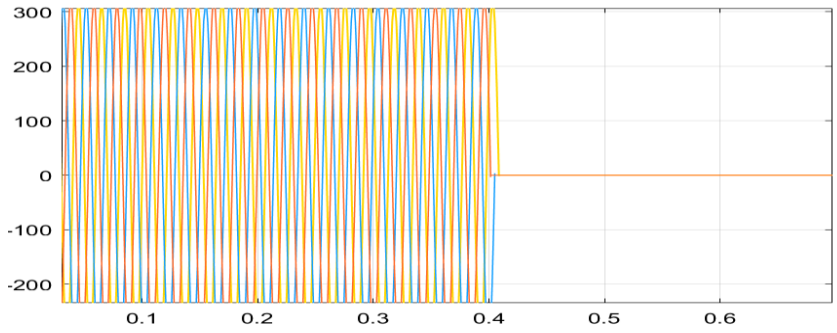

Figure 55. Grid disconnection after the frequency relay (Tan, 2021).

6.3.2 Over frequency test results

A frequency variation event of 53 Hz was achieved by emulating the frequency of the system to a value of 53 Hz, as illustrated in Figure 56. The frequency relay was configured to operate when the over-frequency condition reaches 52.5 Hz. Upon reaching this threshold, the frequency relay will send a signal to activate the three-phase circuit breaker and disconnect the grid. In this case, the delay was set to 0.40 seconds. Therefore, the grid was disconnected in 0.4 seconds, as illustrated in Figure 55 (Tan, 2021).

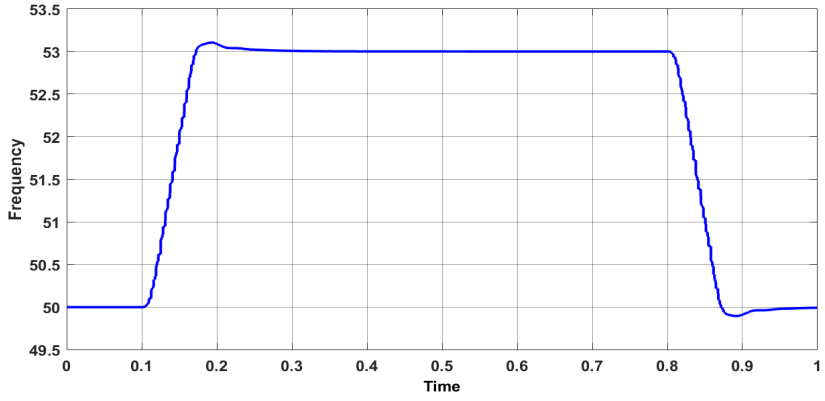

Figure 56. frequency reaches 53 Hz which activates the frequency relay (Tan, 2021).

6.4 Real-time simulation - OPAL-RT

The offline simulation involves creating a power system model and control system in a simulation environment, such as Simulink. The main advantage is the ability to test the system algorithms without the need for external software or hardware connections (Memon, 2024). However, utilizing real-time simulation and hardware-in-the-loop enhances the efficiency in engineering applications such as electrical and electronics applications (Mohanty et al., 2018). The real-time simulator primarily utilizes tools from the distributed package, such as RT-LAB and dSPACE, which offer unique specifications and tools. RT-LAB is real-time simulation software fully compatible with the MATLAB environment. The strength of this technology is its flexibility, which allow it to be utilized in various systems and control applications (Mohanty et al., 2018).

Innovations in computing hardware have led to the development of simulation tools with better performance and lower cost (Mohanty et al., 2018). Real-time simulation involves using a fixed time step (TS) that matches the real-world clock rate. Therefore, the simulation results are presented in discrete-time intervals. Real-time simulation is a discrete time electromagnetic transient simulator. Additionally, performing real-time simulation testing consists of offline simulation, software-in-the-loop, control hardware-in-the-loop, and power system-in-the-loop (Memon, 2024).

The speed and accuracy of the real-time simulation are significantly dependent on the test step size. The smaller the step size, the greater the accuracy of the output signal. To meet the condition of the real-time simulation, the execution time must be shorter or equal to the step size chosen in the system. Real-time simulators have been significantly developed compared to the previous analog simulators. Currently, digital simulators based on the digital signal processor are the most popular and widely used (Memon et al., 2021).

To enable the enable real-time software-in-the-loop simulation using OPAL-RT, a series of modifications were implemented. The first step was to use a fixed-step solver and the

sample time Ts to the value required by the simulation model. Additionally, create a subsystem that excludes the inputs and outputs. The subsystem must start with the prefix "SM" followed by any chosen name, such as “SM” followed by a chosen name such as “SM_ModelName, which is responsible for compiling or processing code within the simulation setup. Additionally, another subsystem was created to manage the inputs and outputs that is the interface, with the name starting with the prefix "SC" (Barrios-Gomez et al., 2020). A model initialization block was then added to set the sample time required for the simulation model, which is in this case it was 250 microseconds, as illustrated in Figure 56.

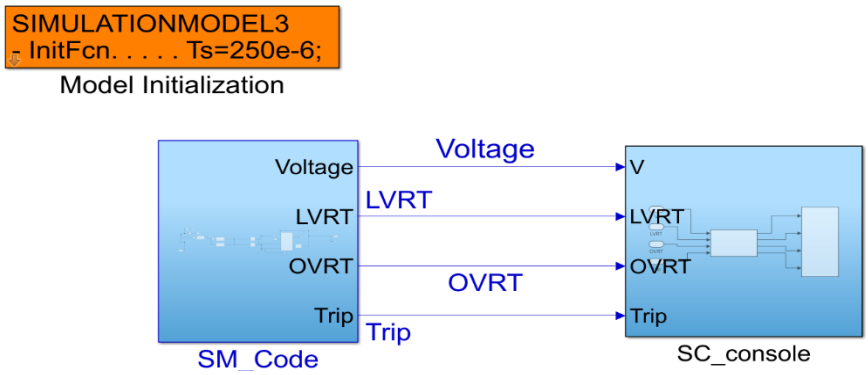

Figure 57. Real-time simulation model.

The initialization block includes several functions such as the preload function that runs before the model loads, to set up the environment or workspace variables. The initial function is used to initialize the variable of the simulation model. Post load Function executes after the model loads, used for additional setup tasks. The Start function executes at the start of the simulation for tasks like opening files or initializing hardware.

The opComm block must be added from the RT lab library to exchange signals between the subsystems of the model. This block also runs the computation between the subsystems in OPAL-RT's real-time simulation platform, and the console (GUI) to ensure seamless communication within the model.

The key parameters of the OpCOmm block in Figure 57 include specifying the number of inputs, this model required four ports. The acquisition group number in the RT-LAB Op-Comm block is used to organize and manage data acquisition in the simulation, while enable synchronization is used to ensure that the data received by the signal is synchronized with the real-time clock. Enable interpolation to allow the interpolation of the data to match the sample time. The threshold time between host and target to ensure that the simulation remains within the acceptable time limits, usually it set to one second to ensure that the host and the target are not differ by more than one second.

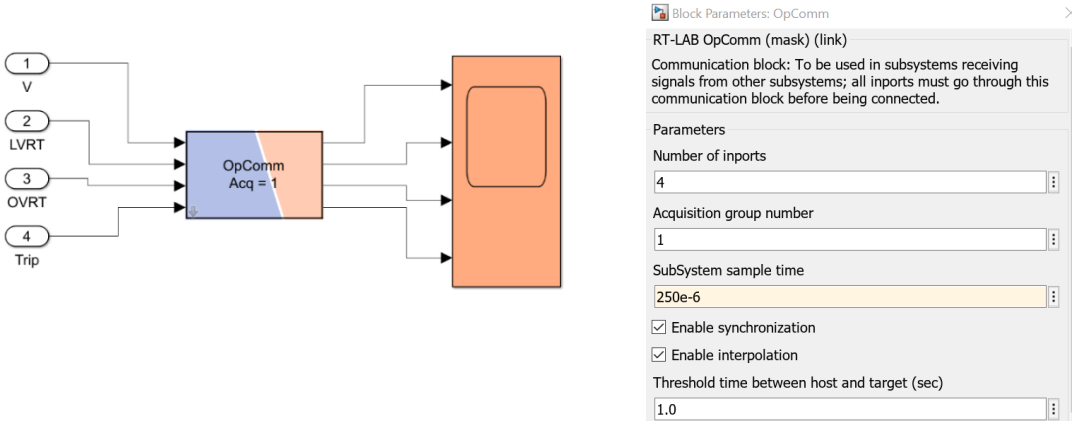

Figure 58. Opcomm block.

As illustrated in Figure 58, the target setup utilizing the OP4510 real-time simulator was established in the FREESI (Future Reliable Electrical and Energy Systems Integration) laboratory at the University of Vaasa, Finland. OP4510 is a comprehensive simulation system with Kintex 7 FPGA. It includes a robust target computer along with a high-speed processor (OPAL-RT Technologies. (n.d.).

Figure 59. OPAL-RT setup.

The x-axis in Figure 59 represents the time in seconds, while the y-axis is the voltage per unit (p.u.). The graph illustrates the voltage signal from the device under the test, which is in this situation the signal from the inverter (green line), UVRT thresholds (red line), and trip signal (purple line). When the voltage signal violates the UVRT threshold, the trip signal will switch from zero to 1, which indicates that the inverter should be disconnected from the grid. Otherwise, the trip signal will remain at zero, which indicates the ability of the inverter to remain connected to the grid. The graph illustrates the voltage signal, OVRT thresholds, and trip signal. The "opComm" indicates that the data is being communicated as a part of the real-time execution process, which can be used to send data from the Simulink model to another hardware or software connected to the OPAL-RT.

In this OVRT scenario, the voltage started at the nominal operating level for 10 seconds. Then the voltage increased from the nominal value to 1.13 p.u. and sustained for a duration of 50 seconds. As illustrated in the graph, the voltage crossed the OVRT threshold. Therefore, as per the OVRT graph, the grid should be capable of remaining connected. Therefore, the trip signal did not operate.

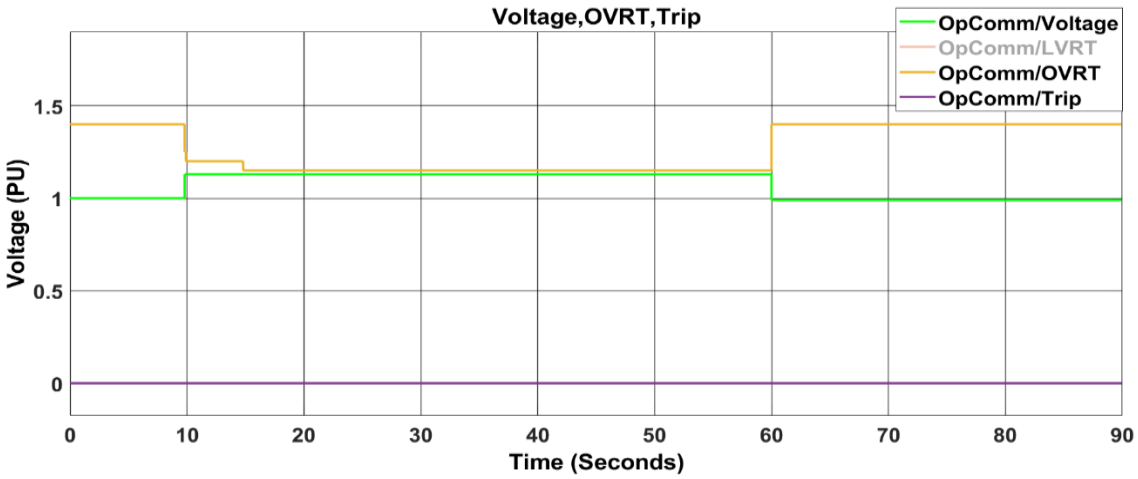

Figure 60. Real-time simulation 1.13 p.u. for 50 seconds.

The x-axis in Figure 60 represents the time in seconds, while the y-axis is the voltage per unit (p.u.). The graph illustrates the voltage signal from the device under the test, which is in this situation the signal from the inverter (green line), UVRT thresholds (red line), and trip signal (purple line). When the voltage signal violates the UVRT threshold, the trip signal will switch from zero to 1, which indicates that the inverter should be disconnected from the grid. Otherwise, the trip signal will remain at zero, which indicates the ability of the inverter to remain connected to the grid. The graph illustrates the voltage signal, OVRT thresholds, and trip signal. In the OVRT test scenario depicted in Figure 60, the "opComm" indicates that the data is being communicated as a part of the real-time execution process. The voltage started at the nominal operating level for 10 seconds. Then the voltage increased from the nominal value to 1.17 p.u. and sustained for a duration of 50 seconds. As illustrated in the graph, the voltage crossed the OVRT threshold. Therefore, the generating modules should be disconnected, and as expected, the trip function was activated exactly at the moment when the voltage signal violated the UVRT threshold.

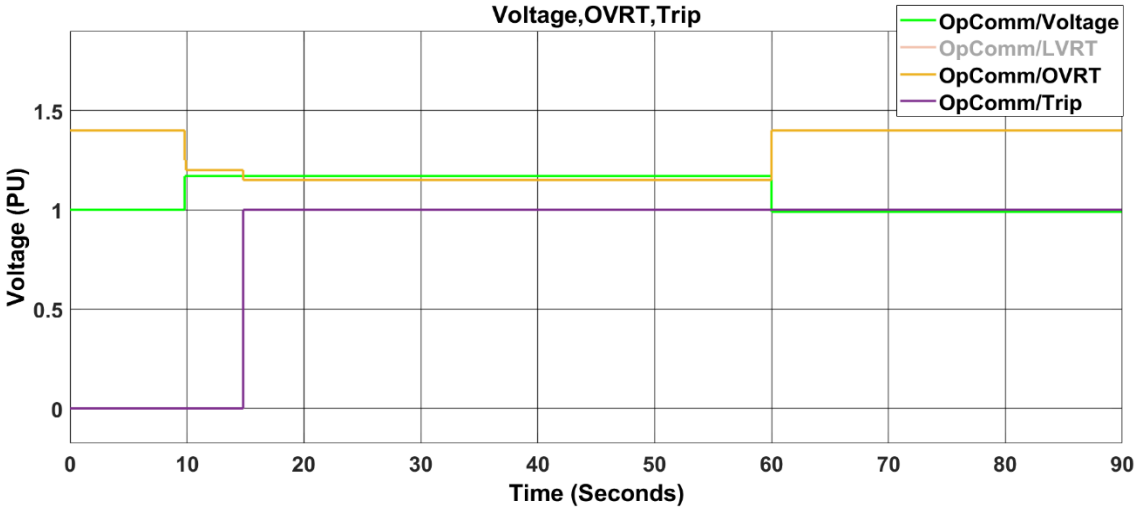

Figure 61. Real-time simulation 1.17 p.u. for 50 seconds.

In Figure 61, the "opComm" indicates that the data is being communicated as a part of the real-time execution process, which can be used to send data from the Simulink model to another hardware or software connected to the OPAL-RT. In the UVRT test scenario illustrated, the voltage started at the nominal operating level for 2 seconds. Then a fault occurs and causes a decrease in the voltage from the nominal value to 0.6 p.u. and sustained for a duration of less than 1 second. The voltage signal falls close to the UVRT threshold but does not violate it. Therefore, the inverter should be capable of remaining connected; as illustrated in the graph, the trip signal did not operate.

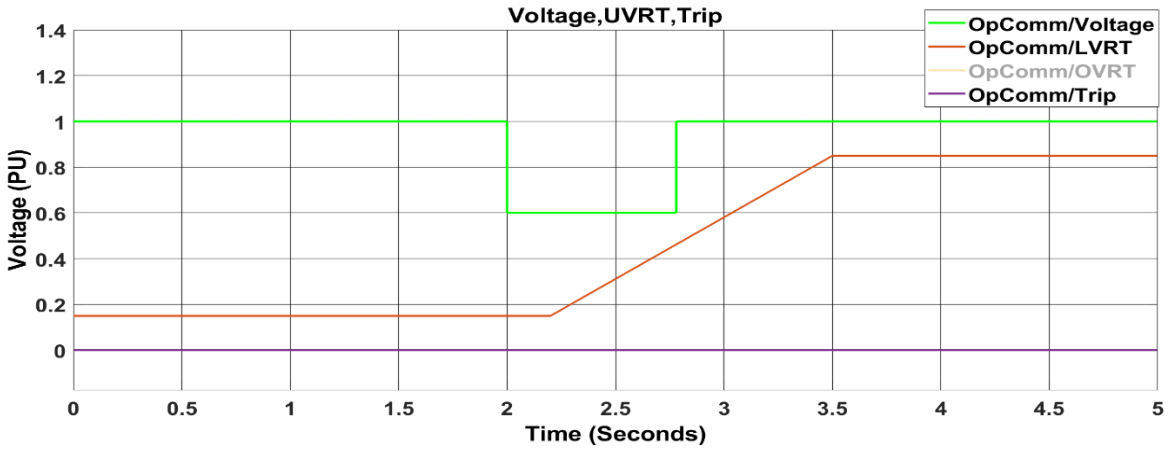

Figure 62. Real-time simulation 0.6 p.u. for less than one seconds.

The x-axis in Figure 62 represents the time in seconds, while the y-axis is the voltage per unit (p.u.). The graph illustrates the voltage signal from the device under the test, which is in this situation the signal from the inverter (green line), UVRT thresholds (red line), and trip signal (purple line). When the voltage signal violates the UVRT threshold, the trip signal will switch from zero to 1, which indicates that the inverter should be disconnected from the grid. Otherwise, the trip signal will remain at zero, which indicates the ability of the inverter to remain connected to the grid. The graph illustrates the voltage signal, OVRT thresholds, and trip signal.

The "opComm" depicted in Figure 62 indicates that the data is being communicated as a part of the real-time execution process, which can be used to send data from the Simulink model to another hardware or software connected to the OPAL-RT. The voltage In the UVRT test scenario, started at the nominal operating level for 2 seconds. Then, a fault occurs and causes a decrease in voltage from nominal value to 0.6 p.u., for more than one second. As illustrated in the graph, the voltage dropped below the UVRT region. In this case, the generating modules must be disconnected. Therefore, the trip signal was activated exactly when the voltage signal violated the UVRT threshold.

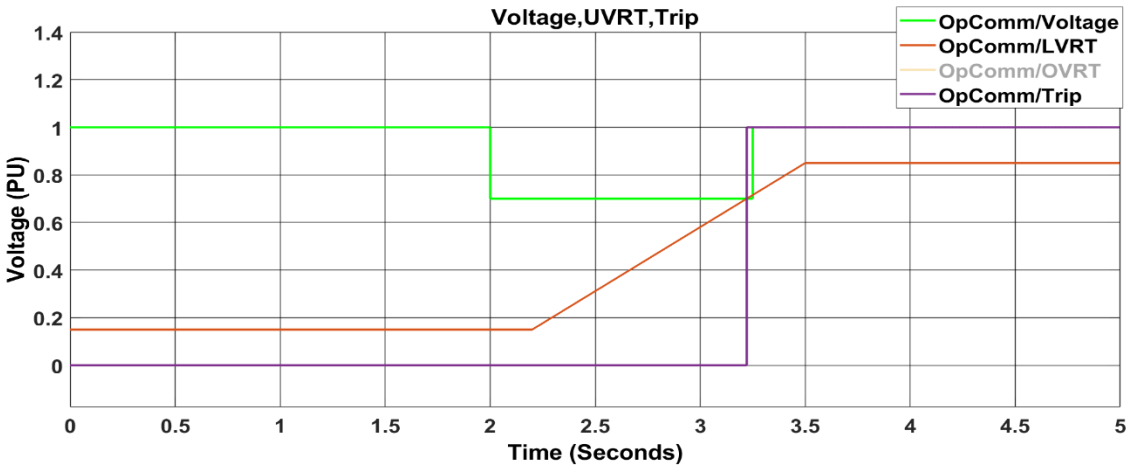

Figure 63. Real-time simulation 0.7 p.u. for 1.25 seconds.

7 Conclusion and future work

There has been a global shift towards renewable energy resources in recent years. This provides advantages to the power system as well as the environment. Grid codes and standards have been developed to accommodate the changes and to ensure the overall reliability and stability of the electrical systems.

The grid is considered a complex system that includes interconnected power generating units, such as renewable resources, that have a fluctuating nature. It is crucial to test the compatibility of the renewable energy sources before integrating them into the grid, since they have a major influence that affects the overall reliability of the network. Therefore, grid code compliance testing is a mandatory process when integrating renewable energy resources into the grid to ensure the stability of the electrical system.

This master thesis provides a comprehensive simulation process for testing the grid code compliance using MATLAB Simulink, which is considered a safe and efficient alternative method compared to the traditional on-site testing methods that are often time-consuming and costly. The performance of the grid-connected inverter was tested by focusing on various under-voltage ride-through and over-voltage ride-through scenarios, as well as the frequency control tests. The objective is to provide simulation-based grid code compliance testing of the inverter connected to the grid, with a specific emphasis on developing a grid emulator model for grid code compliance.

The initial process involved reviewing EN50549-1, EN50549-2, and EN50549-10 standards, which provide the requirements for the generating plants to be connected in parallel with the distribution networks. Additionally, the focus was to develop a grid emulator model for grid code compliance using MATLAB Simulink.

The aim of the second stage of the thesis was pivotal in the development of a simulation to test grid compliance using MATLAB Simulink. The focus was on key factors such as UVRT and OVRT. The goal was achieved by conducting different scenarios of the output

signal of the grid-tied inverter, then comparing them with the predefined thresholds. To evaluate the performance of the simulation model, the voltage-time curves were divided into three zones, and at least two tests were conducted within each zone to verify the compatibility with the threshold based on the EN50549-1, EN50549-2, and EN50549-10 standards.

The final stage involved modification of the simulation model to be able to run the model in real-time using the OPAL-RT real-time simulator. This step is essential for evaluating the performance and reliability of the grid compliance of the simulation model. Additionally, survey the current HIL approaches for testing grid code compliance. The aim was to collect previous research papers that conducted relevant grid code compliance testing frameworks such as under-voltage ride-through and over-voltage ride-through, utilizing offline or real-time simulation. The focus was on the ability of the generating modules to withstand the variations in voltage and frequency thresholds to identify the practices that could be employed to improve the existing framework of this thesis.

In the future, the developed methodology and models will be utilized to test Danfoss inverter, utilizing Power Hardware-in-the-Loop testing with the emulator in the FREESI laboratory at the University of Vaasa. Additionally, in the simulation model presented in this thesis, the trip signal is simulated and ideal, used only to demonstrate the testing procedure. However, during real inverter testing, the trip signal must originate from the actual inverter.

Furthermore, the compliance testing process developed and tested in this thesis was based on ideal three-phase faults. Non-ideal conditions that introduce complexities such as two-phase faults, transients, harmonics, or noise could significantly impact the accuracy of these detection processes, which will affect the evaluation of grid code compliance. Therefore, future work will include the testing process under non-ideal conditions to ensure the accuracy of the compliance evaluations in real-world scenarios.

References

Abed, A. M., Alkhazraji, A. A., & Al-Kubragyi, S. S. A. (2023). Modelling and simulation of an on grid 100-kW photovoltaic system. *International Journal of Power Electronics and Drive Systems*, *14*(3), 1651–1659. https://doi.org/10.11591/ijpeds.v14.i3.pp1651-1659

Ahmed, F., Al Kez, D., McLoone, S., Best, R. J., Cameron, C., & Foley, A. (2023). Dynamic grid stability in low carbon power systems with minimum inertia. *Renewable Energy*, *210*, 486–506. https://doi.org/https://doi.org/10.1016/j.renene.2023.03.082

Akanto, J. M., Hazari, M. R., & Mannan, M. A. (2021). Lvrt and stability enhancement of grid-tied wind farm using dfig-based wind turbine. *Applied System Innovation*, *4*(2). https://doi.org/10.3390/asi4020033

Albu, M., Dumitrescu, A.-M., & Popovici, R. (2014). Rate of change of frequency - a power quality descriptor. *2014 16th International Conference on Harmonics and Quality of Power (ICHQP)*, 312–316. https://doi.org/10.1109/ICHQP.2014.6842900

Ali Memon, A. (n.d.). *Communication-Based Adaptive Protection of AC Microgrids with Converter-Based Distributed Energy Resources ~~~ ACTA WASAENSIA 529*. https://urn.fi/URN:ISBN:978-952-395-131-0

Barrios-Gomez, J. A., Sanchez, F., Claudio, G., Gonzalez-Longatt, F., Acosta, M. N., Denysiuk, S., & Strelkova, H. (2020). Framework for Real-Time Simulation of Hardware in the Loop Applied to Primary Frequency Control. *2020 IEEE 7th International Conference on Energy Smart Systems, ESS 2020 - Proceedings*, 30–35. https://doi.org/10.1109/ESS50319.2020.9160023

Corporation, M. (n.d.). *Park, Inverse Park and Clarke, Inverse Clarke Transformations MSS Software Implementation User Guide Park, Inverse Park and Clarke, Inverse Clarke Transformations MSS Software Implementations User Guide Park, Inverse Park and Clarke, Inverse Clarke Transformations MSS Software Implementations User Guide 3*.

Cui, T., Liang, J., Liu, S., Dong, J., Li, X., & Li, A. (2022). Research on PV Low Voltage Ride-Through Control Based on RT-LAB Hardware-in-the-Loop. *2022 China International Conference on Electricity Distribution (CICED)*, 1299–1304. https://doi.org/10.1109/CICED56215.2022.9929203

Drechsler, M. F., Seifert, G., Peintner, J., Reway, F., Riener, A., & Huber, W. (2022). *How Simulation based Test Methods will substitute the Proving Ground Testing?* https://doi.org/10.1109/IV51971.2022.9827394

Etxegarai, A., Torres, E., Zamora, I., San Martin, J. I., & Eguia, P. (2014). Review of procedures for verification of grid code compliance of renewable generation. *Renewable Energy and Power Quality Journal*, *1*(12), 855–861. https://doi.org/10.24084/repqj12.512

Flores, L. I. R., & Loaeza, H. J. M. (2022a). Grid Code, Part 2: Electrical Parameterization and Global Comparison in the Energy Sector. *Proceedings of the 2022 IEEE 40th Central America and Panama Convention, CONCAPAN 2022*. https://doi.org/10.1109/CONCAPAN48024.2022.9997702

Flores, L. I. R., & Loaeza, H. J. M. (2022b). Grid Code, Part 2: Global Parameterization and Comparison in the Electricity Sector. *2022 IEEE PES Generation, Transmission and Distribution Conference and Exposition – Latin America (IEEE PES GTD Latin America)*, 1–8. https://doi.org/10.1109/IEEEPESGTDLatinAmeri53482.2022.10037781

Foqha, T., Alsadi, S., Refaat, S. S., & Abdulmawjood, K. (2023). Experimental Validation of a Mitigation Method of Ferranti Effect in Transmission Line. *IEEE Access*, *11*, 15878–15895. https://doi.org/10.1109/ACCESS.2023.3244826

Fingrid. (2018). *Grid code specifications for power generating facilities VJV2018*. Fingrid. https://www.fingrid.fi/en/grid/grid-connection-agreement-phases/grid-code-specifications/grid-code-specifications-for-power-generating-facilities2/

Finnish Standardization Association SFS ry. (2022). SFS-EN 50549-10:2022: Requirements for generating plants to be connected in parallel with distribution networks: Part 10, Tests for conformity assessment of generating units (2022-11-11). Finnish Standardization Association SFS ry.

Hadjidemetriou, L., Demetriou, P., & Kyriakides, E. (2015). Investigation of different Fault Ride Through strategies for renewable energy sources. *2015 IEEE Eindhoven PowerTech*, 1–6. https://doi.org/10.1109/PTC.2015.7232594

Hafezi, H., Laaksonen, H., Kauhaniemi, K., Lauttamus, P., & Strandberg, S. (2021). *Power Electronic Converters Simulation Model Verification for Grid Code Compliance Testing*. https://doi.org/10.1109/ISGTEurope52324.2021.9639983

Hassan, S. J. U., Mehdi, A., Haider, Z., Song, J.-S., Abraham, A. D., Shin, G.-S., & Kim, C.-H. (2024). Towards medium voltage hybrid AC/DC distribution Systems: Architectural Topologies, planning and operation. *International Journal of Electrical Power & Energy Systems*, *159*, 110003. https://doi.org/https://doi.org/10.1016/j.ijepes.2024.110003

Haupala, N., & Bhumkittipich, K. (2019). Improvement of Low Voltage Ride-through Capability of DFIG-based Wind Turbines under Low Voltage Condition. *2019 7th International Electrical Engineering Congress (IEECON)*, 1–4. https://doi.org/10.1109/iEECON45304.2019.8938884

IEA. (2023). *Wind power capacity in the Net Zero Scenario, 2015-2030, IEA, Paris*. https://www.iea.org/data-and-statistics/charts/wind-power-capacity-in-the-net-zero-scenario-2015-2030

International Renewable Energy Agency. (2024). *International Renewable Energy Agency (2023) – processed by Our World in Data. "Solar energy capacity" [dataset]. International Renewable Energy Agency, "Renewable Electricity Capacity and Generation Statistics" [original data].*

Istardi, D., Halim, B., & Febriansyah, A. J. (2017). High Efficiency Single Phase Inverter Design. *Proceeding of the Electrical Engineering Computer Science and Informatics*, *4*(1). https://doi.org/10.11591/eecsi.v4.998

Khan, B., Guerrero, J., Padmanaban, S., Alhelou, H. H., Mahela, O. P., & Tanwar, S. (2021). *Active electrical distribution network : a smart approach*. John Wiley & Sons, Inc.

Laine, H. (2020). *Grid code compliance testing using HIL system* (Master's thesis, Tampere University). Retrieved from https://trepo.tuni.fi/bitstream/handle/10024/120531/LaineHenri.pdf?sequence=2

LeSage, J. (2024). *Grid Code Compliance for Renewable Resource Integration* https://github.com/jonlesage/Grid-Codes/releases/tag/v19.2.0

Letaief, F., Hamouda, M., & Al-Haddad, K. (2023). Review and Discussion of Recent Codes for Inverter-Based RESs and PPMs Under Grid Voltage Sag Conditions. *2023 IEEE International Conference on Artificial Intelligence and Green Energy, ICAIGE 2023*. https://doi.org/10.1109/ICAIGE58321.2023.10346391

Li, C., Wu, Y., Sun, Y., Zhang, H., Liu, Y., Liu, Y., & Terzija, V. (2020). Continuous Under-Frequency Load Shedding Scheme for Power System Adaptive Frequency Control. *IEEE Transactions on Power Systems*, *35*(2), 950–961. https://doi.org/10.1109/TPWRS.2019.2943150

Li, Z., Wu, F., Xu, L., & Niu, C. (2019). Research on different topologies of over-voltage-ride-through testing device for PV power generation. https://doi.org/10.1049/cp.2019.0638

Liu, H. (2016). Control Design of a Single-Phase DC/AC Inverter for PV Applications. http://scholarworks.uark.edu/etdhttp://scholarworks.uark.edu/etd/1618

Lone, A. H., Ishwarrao Gedam, A., & Sekhar, K. R. (2023). Fault Ride Through with Con-formance to Grid Voltage Limits in Photovoltaic Grid Connected Inverters. https://doi.org/10.1109/GlobConET56651.2023.10150098

Magnago, H., Figueira, H., Gagrica, O., & Majstorovic, D. (2021). HIL-based certification for converter controllers: Advantages, challenges and outlooks (Invited Paper). Proceedings of 2021 21st International Symposium on Power Electronics, Ee 2021. https://doi.org/10.1109/Ee53374.2021.9628196

Mahela, O. P., Gupta, N., Khosravy, M., & Patel, N. (2019). Comprehensive overview of low voltage ride through methods of grid integrated wind generator. IEEE Access, 7, 99299–99326. https://doi.org/10.1109/ACCESS.2019.2930413

Memon, A. A., Laaksonen, H., & Kauhaniemi, K. (2021). Microgrid Protection with Conventional and Adaptive Protection Schemes. In A. Anvari-Moghaddam, H. Abdi, B. Mohammadi-Ivatloo, & N. Hatziargyriou (Eds.), Microgrids: Advances in

Operation, Control, and Protection (pp. 523–579). Springer International Publishing. https://doi.org/10.1007/978-3-030-59750-4_19

Memon, AA, University, V., Vaasa, U. o., & https://orcid.org/0000-0003-1290-6312. (2024). Communication-Based Adaptive Protection of AC Microgrids with Converter-Based Distributed Energy Resources . University of Vaasa.

Menegazzo, L. F. R., Severo, A. L. N., Bortolini, R. J. F., Magnago, H., Carnielutti, F. M., Bellinaso, L. V, Michels, L., & Pinheiro, H. (2021). Hardware-in-the-Loop Low Voltage Fault Ride Through Tests of Commercial Photovoltaic Inverters. 2021 Brazilian Power Electronics Conference (COBEP), 1–8. https://doi.org/10.1109/COBEP53665.2021.9684133

Miyagi, D., Sato, R., Ishida, N., Sato, Y., Tsuda, M., Hamajima, T., Shintomi, T., Makida, Y., Takao, T., & Iwaki, K. (2015). Experimental Research on Compensation for Power Fluctuation of the Renewable Energy Using the SMES Under the State-of-Current Feedback Control. IEEE Transactions on Applied Superconductivity, 25(3), 1–5. https://doi.org/10.1109/TASC.2014.2368051

Mohanty, A., Viswavandya, M., Ray, P. K., & Mohanty, S. (2018). Literature survey on OPAL-RT Technologies with Advance features and Industrial applications. 2018 1st International Conference on Advanced Research in Engineering Sciences (ARES), 1–5. https://doi.org/10.1109/ARESX.2018.8723268

Niklas Modig Robert Eriksson Pia Ruokolainen Jon Nerbø Ødegård Simon Weizenegger Thomas Dalgas Fechtenburg Svenska kraftnät Svenska kraftnät Fingrid Statnett Statnett Energinet, A. (2022). Overview of Frequency Control in the Nordic Power System.

Niu, L., Wang, X., Wu, L., Yan, F., Xu, M., & Hu, X. (2018). Low Voltage Ride-through Strategy for Wind Farm and VSC-HVDC. 2018 International Conference on Power System Technology (POWERCON), 2183–2188. https://doi.org/10.1109/POWERCON.2018.8602163

OPAL-RT Technologies. (n.d.). RT-LAB / RCP / HIL System OP4510 Simulator [Description of simulator]. Retrieved from https://www.opal-rt.com/products/rt-lab/

Parvez, M., Elias, M. F. M., Rahim, N. A., & Osman, N. (2016). Current control techniques for three-phase grid interconnection of renewable power generation systems: A review. Solar Energy, 135, 29–42. https://doi.org/10.1016/j.solener.2016.05.029

Padmanaban, S., Chenniappan, S., & Palanisamy, S. (2023). Grid interconnection standards, grid code requirements and compliance for renewable integration. https://doi.org/10.1016/B978-0-443-15578-9.00007-8

Rafiq, M. U., Pugliese, S., & Liserre, M. (2022). Modeling of Symmetrical and Asymmetrical Grid Faults for P-HIL Accuracy Analysis in LVRT Tests. *2022 IEEE Energy Conversion Congress and Exposition, ECCE 2022*. https://doi.org/10.1109/ECCE50734.2022.9947802

Requirements for Generating Plants to be Connected in Parallel With Distribution Networks. Part 2: Connection to a MV Distribution Network. Generating Plants up to and Including Type B, Standard SFS-EN 50549-2:2019, Eur. Committee Electrotechnical Standardization, Brussels, Belgium, Feb. 2019

Requirements for Generating Plants to be Connected in Parallel With distribution Networks. Part 1: Connection to a LV Distribution Network. Generating Plants up to and Including Type B, Standard SFS-EN 50549- 1:2019, Eur. Committee for Electrotechnical Standardization, Brussels, Belgium, Feb. 2019

Rietveld, G., Wright, P. S., & Roscoe, A. J. (2020). Reliable Rate-of-Change-of-Frequency Measurements: Use Cases and Test Conditions. *IEEE Transactions on Instrumentation and Measurement*, *69*(9), 6657–6666. https://doi.org/10.1109/TIM.2020.2986069

Rodney Tan. (2021, June 9). *Frequency Relay Block*. MATLAB Central File Exchange. https://www.mathworks.com/matlabcentral/fileexchange/64572-frequency-relay-block

Roos, P. (2020). *A Comparison of Grid-Forming and Grid-Following Control of VSCs*. http://www.teknat.uu.se/student

Sathiyanarayanan, T., & Vijay M., D. (2024). Chapter 5 - Grid interconnection standards, grid code requirements and compliance for renewable integration. In S. Chenniappan, S. Padmanaban, & S. Palanisamy (Eds.), *Power Systems Operation with*

100% Renewable Energy Sources (pp. 55–64). Elsevier. https://doi.org/https://doi.org/10.1016/B978-0-443-15578-9.00007-8

Shanmugam, K., Pitto, G., & Barbato, L. (2020). Gridcode compliances and Operational Requirements of Grid connected BESS-Reneweable Power Plants. *2020 IEEE International Conference on Power Systems Technology (POWERCON)*, 1–6. https://doi.org/10.1109/POWERCON48463.2020.9230534

Stockl, J., Miletic, Z., Bnundlinger, R., Schulz, J., Ablinger, R., Tremmel, W., & Johnson, J. (2018). Pre-evaluation of grid code compliance for power electronics inverter systems in low-voltage smart grids.

Wenrui, H., Li, W., & Hongli, Z. (n.d.). *Extraction method of renewable energy output interval based on CLIQUE clustering*.

Xu, S., Xue, Y., & Chang, L. (2021). Review of Power System Support Functions for Inverter-Based Distributed Energy Resources-Standards, Control Algorithms, and Trends. In *IEEE Open Journal of Power Electronics* (Vol. 2, pp. 88–105). Institute of Electrical and Electronics Engineers Inc. https://doi.org/10.1109/OJPEL.2021.3056627

Zhang, J., Zhang, N., & Ge, Y. (2023). Energy Storage Placements for Renewable Energy Fluctuations: A Practical Study. *IEEE Transactions on Power Systems*, *38*(5), 4916–4927. https://doi.org/10.1109/TPWRS.2022.3214983

Zhang, J., Zheng, F., Zhang, X., Huang, J., Wang, W., Gao, F., & Tan, W. (2016). The setup of a flexible test bench for the low-voltage-ride-through capability of solar energy converter. *2016 IEEE 8th International Power Electronics and Motion Control Conference (IPEMC-ECCE Asia)*, 2765–2769. https://doi.org/10.1109/IPEMC.2016.7512735

Appendices

Appendix 1. Voltage versus frequency MATLAB function

```
function N50549(V, F, t)

     persistent mustPlot mayPlot vfPlot;

     % Ride-through criteria for UVRT and OVRT
     LVRT.T = [-1     0   0+1e-6    0.2     1.5       3    1000];
     LVRT.V =  [0.15   0.15   0.15     0.15  0.85   0.85   0.85];
     % Fixed values for LVRT
     OVRT.T = [-1     0    0+1e-6  0.1   0.1+1e-6   5
         5+1e-6  60    60+1e-6 600];
     OVRT.V = [1.4      1.4      1.25   1.25     1.20    1.20   1.15
         1.15      1.10 1.10];

  if isempty(mustPlot)
    figure(1); hold on;
    % Plot voltage ride-through boundaries
  mustPlot = plot([LVRT.T(1) LVRT.T(1) LVRT.T(4) LVRT.T(4) LVRT.T(1)],...
   [LVRT.V(1) LVRT.V(4) LVRT.V(4) LVRT.V(1) LVRT.V(1)],'r','LineWidth',2);
mayPlot = plot([LVRT.T(1) LVRT.T(1) OVRT.T(1) OVRT.T(1) OVRT.T(5) OVRT.T(5)
...
    LVRT.T(1)],...
        [OVRT.V(1) LVRT.V(1) LVRT.V(1) OVRT.V(1) OVRT.V(5) LVRT.V(1) ...
        LVRT.V(1)],  'y','LineWidth',2);

    plot([47 53 53 47 47],[0.15 0.15 1.2 1.2 0.15], ...
        'Color',[0.8824    0.5333    0.4627],'LineWidth',2);
    % Plot dotted lines
    plot([50 50],[0.15 1.2],'k--');
    plot([47 53],[1 1],'k--');
    % Plot initial voltage-frequency point
    vfPlot = plot(F,V,'ro');

    hold off; grid on;
    xlim([47 53]);
    ylim([0.15 1.2]);

    xlabel('Frequency (Hz)'); ylabel('Voltage (pu)');
    title('EN50549-1 EN50549-2 & EN5049-10 Ride Through Requirements');
    else
    set(vfPlot,'XData',F,'YData',V);
    pause(0.01);
    end

    pause(0.01);
    end
```